





Article

Halogenated Pyrrolopyrimidines with Low MIC on *Staphylococcus aureus* and Synergistic Effects with an Antimicrobial Peptide

Cecilie Elisabeth Olsen ¹, Fredrik Heen Blindheim ¹, Caroline Krogh Sogaard ², Lisa Marie Røst ³ , Amanda Holstad Singleton ², Olaug Elisabeth Torheim Bergum ², Per Bruheim ³ , Marit Otterlei ² , Eirik Sundby ⁴ and Bård Helge Hoff ^{1,*} 

- ¹ Department of Chemistry, Norwegian University of Science and Technology (NTNU), NO-7491 Trondheim, Norway; cecilie.e.olsen@ntnu.no (C.E.O.); fredrik.h.blindheim@ntnu.no (F.H.B.)
- ² Department of Clinical and Molecular Medicine, Norwegian University of Science and Technology (NTNU), NO-7489 Trondheim, Norway; caroline.d.sogaard@ntnu.no (C.K.S.); amanda.singleton@ntnu.no (A.H.S.); olaug.e.t.bergum@ntnu.no (O.E.T.B.); marit.otterlei@ntnu.no (M.O.)
- ³ Department of Biotechnology and Food Science, Norwegian University of Science and Technology (NTNU), NO-7491 Trondheim, Norway; lisa.m.rost@ntnu.no (L.M.R.); per.bruheim@ntnu.no (P.B.)
- ⁴ Department of Material Science, Norwegian University of Science and Technology (NTNU), NO-7491 Trondheim, Norway; eirik.sundby@ntnu.no
- * Correspondence: bard.h.hoff@ntnu.no



Citation: Olsen, C.E.; Blindheim, F.H.; Sogaard, C.K.; Røst, L.M.; Singleton, A.H.; Bergum, O.E.T.; Bruheim, P.; Otterlei, M.; Sundby, E.; Hoff, B.H. Halogenated Pyrrolopyrimidines with Low MIC on *Staphylococcus aureus* and Synergistic Effects with an Antimicrobial Peptide. *Antibiotics* **2022**, *11*, 984. <https://doi.org/10.3390/antibiotics11080984>

Academic Editor: Valentina Straniero

Received: 5 July 2022

Accepted: 18 July 2022

Published: 22 July 2022

Publisher's Note: MDPI stays neutral with regard to jurisdictional claims in published maps and institutional affiliations.



Copyright: © 2022 by the authors. Licensee MDPI, Basel, Switzerland. This article is an open access article distributed under the terms and conditions of the Creative Commons Attribution (CC BY) license (<https://creativecommons.org/licenses/by/4.0/>).

Abstract: Currently, there is a world-wide rise in antibiotic resistance causing burdens to individuals and public healthcare systems. At the same time drug development is lagging behind. Therefore, finding new ways of treating bacterial infections either by identifying new agents or combinations of drugs is of utmost importance. Additionally, if combination therapy is based on agents with different modes of action, resistance is less likely to develop. The synthesis of 21 fused pyrimidines and a structure-activity relationship study identified two 6-aryl-7H-pyrrolo [2,3-d] pyrimidin-4-amines with potent activity towards *Staphylococcus aureus*. The MIC-value was found to be highly dependent on a bromo or iodo substitution in the 4-benzylamine group and a hydroxyl in the *meta* or *para* position of the 6-aryl unit. The most active bromo and iodo derivatives had MIC of 8 mg/L. Interestingly, the most potent compounds experienced a four-fold lower MIC-value when they were combined with the antimicrobial peptide betatide giving MIC of 1–2 mg/L. The front runner bromo derivative also has a low activity towards 50 human kinases, including thymidylate monophosphate kinase, a putative antibacterial target.

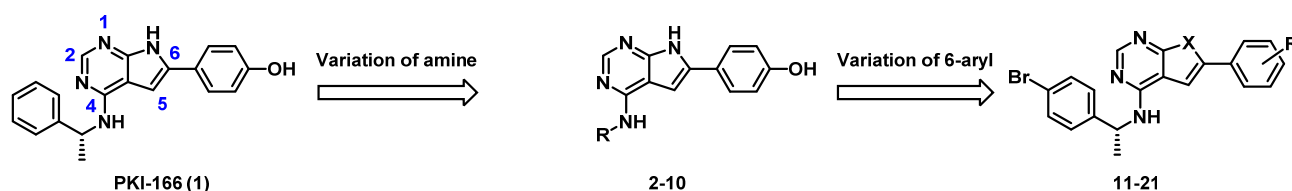
Keywords: antibacterial; pyrrolopyrimidines; synergistic effect; halogenated antibiotic

1. Introduction

Due to the rise in antimicrobial resistance, there is an urgent need of novel antibiotics preferably acting on new biological targets. Moreover, if therapy is based on two or more agents with differing modes of action, resistance is less likely to develop. Several studies have shown a synergistic effect between antimicrobial peptides (AMP) and traditional antibiotics, both in lowering the minimum inhibitory concentration (MIC) and overcoming resistance [1–8]. Synergistic effects can happen by several mechanisms, such as increased uptake [5] or through changes in metabolic nucleotide demand which possibly makes bacteria more sensitive to nucleotide anti-metabolites [6]. We, therefore, wanted to explore this avenue and selected betatide, a cell-penetrating peptide that targets the bacterial DNA sliding clamp [9], which has previously demonstrated substantial MIC lowering when it is combined with classical antibiotics [10].

As a starting point to discover new low molecular weight antibiotics, we selected PKI-166 (Scheme 1), a pyrrolopyrimidine that was previously investigated as an anti-

cancer agent [11] and recently identified as a thymidylate monophosphate kinase inhibitor (TMPK) [12]. Fused pyrimidines in general constitute versatile scaffolds for medicinal chemistry and are present in several FDA-approved drugs [13,14]. They have a bioisosteric relationship to purines and can, therefore, bind to a broad range of proteins [15,16]. Experimental pyrrolopyrimidine antibiotics often inhibit groups of similar bacterial targets [17,18], although some have relatively narrow profiles, such as the inhibitors towards bacterial DNA topoisomerases GyrB and ParE that were developed by Tari et al. [19,20] and the inhibitors of thymidylate monophosphate kinase (TMPK) that was published by Blindheim et al. [12]. TMPK is a key enzyme in the synthesis of thymidine diphosphate, an essential nucleoside in DNA synthesis [21]. This enzyme is located at the junction between the de novo and salvage pathways of thymidine triphosphate synthesis [22], and its inhibition could, therefore, be bactericidal by invoking the thymineless death response [23]. Thymineless death is a phenomenon where bacteria that are starved of thymine nucleosides experience detrimental events, including single- and double-strand DNA-breaks, plasmid elimination, and a loss of transforming ability [23].



Scheme 1. The two stage SAR investigation.

Finally, we wanted to explore the effect of halogen insertion on antibacterial activity. These elements are rarely found in drugs besides X-ray contrast agents [24] and the only heavy halogen-containing drug on the WHO 2021 AWaRe list [25] was brodimoprim [26], which is not in current clinical use [27]. One reason that brominated and iodinated drugs are rare could be that hit selection metrics disfavor these as starting points in drug development campaigns. However, heavier halogen-containing antibiotics have been described from many different origins such as natural products [28,29], by microbial cultivation with halogen salts, [30], and synthetic origin [31–34]. Brominated tryptophanes and tyrosines are also frequently used in peptides with antibiotic effects [35]. Increased activity and stability of heavy halogen-modified peptide antibiotics has also been reported [36]. This effect could be due to the altered size and concomitant change in van der Waals interactions, but could also be caused by directional interactions with the target through halogen bonding [37,38].

Herein we describe a structure-activity relationship study which shows that increased activity and selectivity can be achieved by the insertion of heavy halogens (bromine and iodine). Further, the most active agents in combination with betatide showed a clear synergetic effect towards *S. aureus*. In the search of antibacterial targets, an enzymatic assay towards *E. coli* and human TMPK was performed. Additionally, the most active derivative was evaluated toward a panel of 50 human kinases to identify off-targets.

2. Results

2.1. Study Design

Our previous study attempting to identify *E. coli* TMPK inhibitors revealed that the previously discontinued epidermal growth factor receptor (EGFR) inhibitor PKI-166 [10,12] had an IC_{50} of 15 μ M against *E. coli* TMPK (Scheme 1). We, therefore, wanted to develop this lead further by aiming to (i) reduce the EGFR inhibitory activity, (ii) improve antibacterial activity, and possibly (iii) develop a better structure-activity relationship (SAR) understanding.

From our previous EGFR studies, we knew that the inhibitory activity of this kinase was very sensitive to substitution of the amine part [10]. Therefore, we first investigated variations of the 4-amino group, which led to the discovery that *p*-bromo substitution (compound 5) had improved antibacterial activity with a concomitant reduction in EGFR activity. Then, further SAR investigation was performed by modifying the 6-aryl group

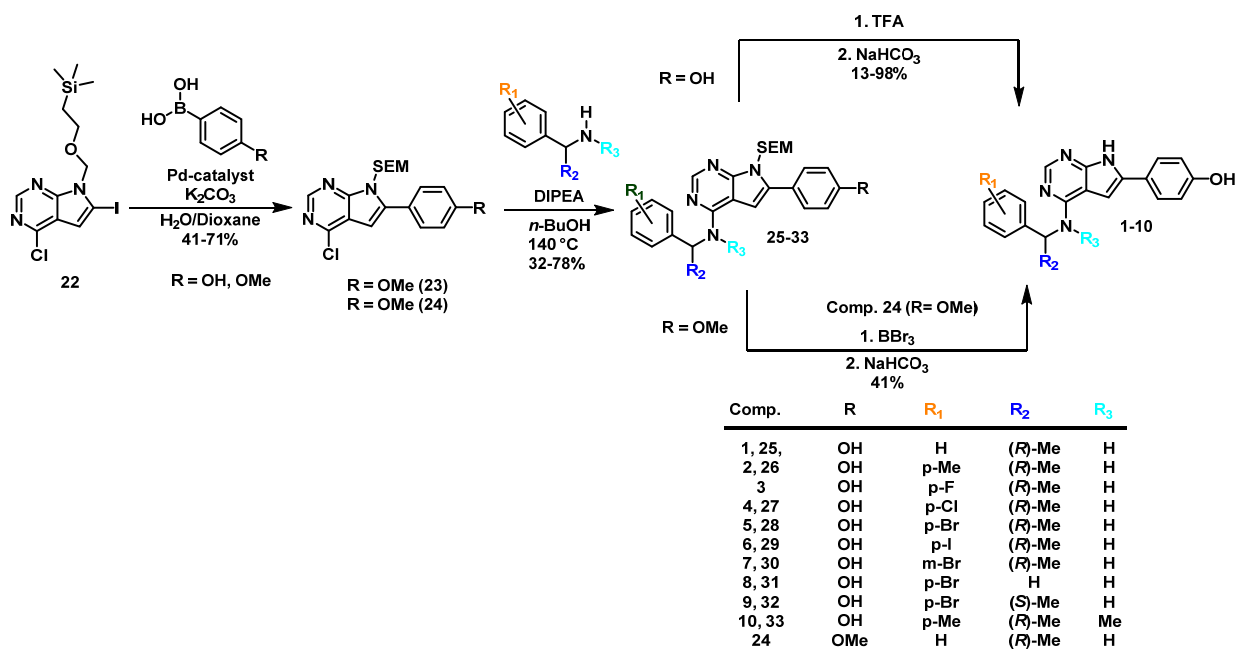
and exchanging the NH in the pyrrolopyrimidine with a sulphur giving the corresponding thienopyrimidine.

In contrast to our previous studies on TMPK inhibitors [10,12] where enzymatic assays were employed, herein we have chosen to assay the compounds in culture to ensure that the cell penetrating compounds are identified. *E. coli* was selected as a model of Gram-negative bacteria and *S. aureus* for Gram-positive bacteria. Finally, we planned to investigate the synergetic effect when combining a small molecular antibiotic with antimicrobial peptides.

2.2. Synthesis of Fused Pyrimidines

The synthesis in the pyrrolopyrimidine series started from 4-chloro-7H-pyrrolo [2,3-*d*]pyrimidine, which was protected with *N*-(trimethyl) silylethoxymethyl (SEM) and selectively iodinated in the 6-position. This yielded building block **22** with two “handles” that could easily be modified in Pd-catalyzed cross-coupling reactions or nucleophilic aromatic substitutions. Compound **22** was then used to construct all pyrrolopyrimidine derivatives.

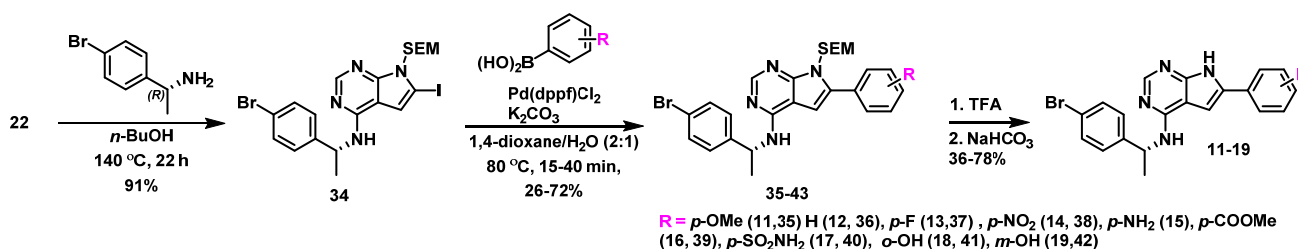
In the first route (Scheme 2), we started with a Suzuki coupling on **22** with 4-hydroxyphenyl boronic acid as coupling partner and Pd₂(dba)₃ as a catalyst. This led to a high selectivity for the mono 6-arylated **23** over the 4,6-diarylated byproduct (19:1 ratio). Yields in the range of 52–71% were obtained. In most cases the aminations at C-4 proceeded smoothly but required significant amounts of co-base when the amine HCl salts were used. Acid catalyzed reactions were unsuccessful. The removal of the SEM-protecting group was then achieved by a two-step protocol using trifluoroacetic acid (TFA) and NaHCO₃ in a previously established procedure [12]. This led to a library of pyrrolopyrimidines in 13–98% yields. Some debenzoylation occurred for the more electron-rich amines, and an overall high crystallinity complicated chromatographic purification. We found purification by reversed phase chromatography to work better than normal phase in most cases. An alternative variant of this route was also evaluated by utilizing the methoxy analog **24**. However, purification after Suzuki coupling was found to be more difficult due to coelution, and the double deprotection at the end both involved the rather harsh reagent boron tribromide and was challenging to monitor by HPLC and ¹H NMR spectroscopy.



Scheme 2. Synthesis of the pyrrolopyrimidines 1–10.

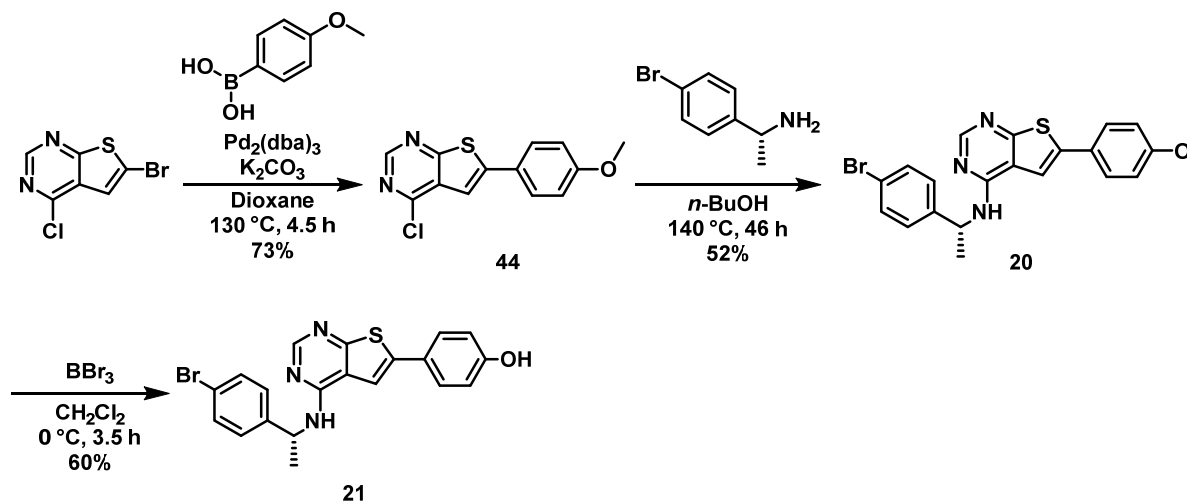
To study the antibacterial effect of varying the 6-aryl substitution pattern, we used the route that is shown in Scheme 3. Here, amination of **22** with the most active amine ((*R*)-1-(4-bromophenyl)ethan-1-amine) gave the advanced building block **34** in 91% yield,

see Scheme 3. In the following chemoselective Suzuki cross-coupling, six different palladium catalysts were evaluated, of which Pd(dppf)Cl₂ was found to be the most selective. Depending on the nature of the substitution and scale, the selectivity varied between 3:1 and 19:1 in favor of the mono-arylated vs. the diarylated by-product and yields in the range of 26–72% were obtained. Finally, SEM deprotection afforded a series of substituted 6-aryl pyrrolopyrimidines in 36–78% yield. The aniline derivative **15** was made by reduction of the nitro analogue **14**.



Scheme 3. Synthesis of the pyrrolopyrimidines **10–20**.

Finally, the effect of substituting the pyrrole nitrogen was investigated by the construction of two thienopyrimidine derivatives. Here, 6-bromo-4-chloro-thienopyrimidine was coupled with 4-methoxyphenyl boronic acid to yield building block **44**, which was aminated with (*R*)-1-(4-bromophenyl)ethan-1-amine to give thienopyrimidine **20**, containing a *para*-methoxy group, see Scheme 4. Demethylation with BBr₃ yielded the corresponding phenolic derivative **21**.



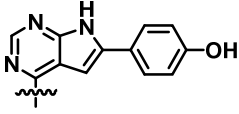
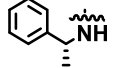
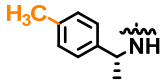
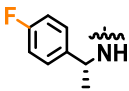
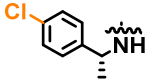
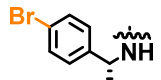
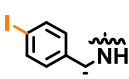
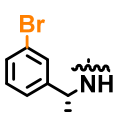
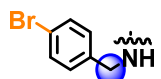
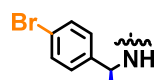
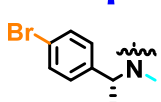
Scheme 4. Synthesis of thienopyrimidines **20** and **21**.

2.3. Evaluation of Antibiotic Activity

2.3.1. Variation of the 4-Amino Group

Our previous efforts at targeting TMPK using enzyme assays have, unfortunately, arrived at compounds that are inactive in culture experiments [12,39]. In this study, we have, therefore, altered our strategy and used minimal inhibitory concentration assays to identify and improve antibacterial agents. A total of 10 pyrrolopyrimidines with variation of the 4-amino group were assayed for their MIC in *E. coli* (MG1655) and *S. aureus* (ATCC29213) using the broth microdilution method [40]. Subsequently, the compounds were also counter-screened for their inhibition of human EGFR. The results are summarized in Table 1.

Table 1. Minimum inhibitory concentration (MIC) in *E. coli* and *S. aureus* and the inhibition of human EGFR for the pyrrolopyrimidines with varied 4-amino group.

Comp.		<i>E. coli</i> MIC [mg/L] ¹	<i>S. aureus</i> MIC [mg/L] ¹	Human EGFR [%] ²
1		>128	64	100
2		>128	16	91
3		>128	>128	92
4		>128	16	91
5		>128	8	81
6		>128	8	43
7		>128	16	89
8		>128	>128	67
9		>128	>128	ND ³
10		>128	>128	16

¹ MIC values were determined using the broth microdilution method [40]. ² Enzymatic EGFR inhibition assay. The compounds were tested towards EGFR using ThermoFisher Z-lyte technology at a concentration of 100 nM. The ATP concentration was equal to KM. ³ Not determined.

Given its activity towards *E. coli* TMPK in enzymatic studies [12], it was unfortunate that **1** and all the other derivatives did not possess any activity towards *E. coli* in culture. This is probably due to the more complex cell wall of Gram-negative bacteria and, therefore, lack of cellular uptake. On the other hand, compound **1** had an MIC of 64 mg/L towards the Gram-positive *S. aureus*. Whereas the corresponding 4-fluoro derivative **3** was inactive, increased potency was seen for the other *para*-substituted derivatives and an MIC of 8 mg/L towards *S. aureus* was seen for the *para*-bromo and *para*-iodo derivatives **5** and **6**. The MIC was increased to 16 mg/L with a *meta*-bromine substituent, which might indicate a steric clash. Interestingly, the removal of the methyl group at the stereocenter (comp. **8**), changing the stereochemistry (comp. **9**) or adding an *N*-methyl (comp. **10**) abolished all activity towards *S. aureus*. The relatively large variation in the MIC values upon these minor structural changes strongly suggests that the compounds act on an intracellular target, rather than having some unspecific effect on the bacterial cell membrane. Finally, the enzymatic assay towards human EGFR showed that the activity dropped when the size of the 4-aryl substituent increased, in line with our earlier assumption.

2.3.2. Variation of the 6-Aryl Group and the 7-Heteroatom

In the second series of potential inhibitors, we varied the 6-aryl group and the heteroatom of the five-membered heterocycle. The results are summarized in Table 2. The pyrrolopyrimidines **11–18** were all inactive towards both *E. coli* and *S. aureus*, but the *meta*-hydroxy derivative **19** had an MIC of 16 mg/L towards *S. aureus*. Further, whereas the methoxy substituted thienopyrimidine **20** had no activity, the corresponding *para*-hydroxy derivative **21** had an MIC of 32 mg/L. This clearly shows the important role of both the pyrrole NH and the *para*- or *meta*-hydroxy group for the activity of this compound class.

Table 2. Minimum inhibitory concentration (MIC) in *E. coli* and *S. aureus* and the inhibition of human EGFR for the 6-aryl substituted pyrrolopyrimidine and thienopyrimidine analogs.

Comp.	6-Aryl	X	<i>E. coli</i> MIC [mg/L] ¹	<i>S. aureus</i> MIC [mg/L] ¹	Human EGFR[% Inhibition] ²
11		NH	>128	>128	-
12		NH	>128	>128	66
13		NH	>128	>128	58
14		NH	>128	>128	33
15		NH	>128	>128	90
16		NH	>128	>128	42
17		NH	>128	>128	85
18		NH	>128	>128	80
19		NH	>128	16	73
20		S	>128	>128	12
21		S	>128	32	5

¹ MIC values were determined using the broth microdilution method [40]. ² Enzymatic EGFR inhibition assay. The compounds were tested towards EGFR using ThermoFisher Z-lyte technology at a concentration of 100 nM. The ATP concentration was equal to K_M .

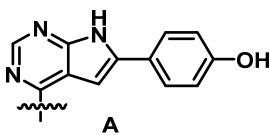
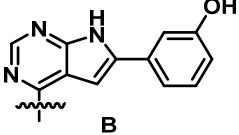
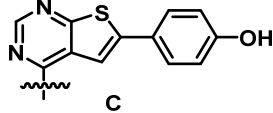
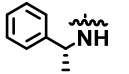
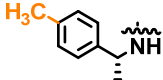
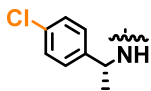
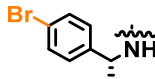
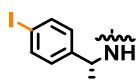
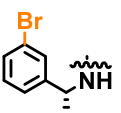
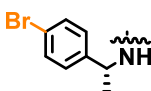
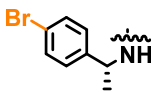
2.3.3. Combination Studies with the Antimicrobial Peptide Betatide

The derivatives with an MIC < 64 mg/L were then subjected to additional MIC profiling towards *S. aureus* in combination with the antimicrobial peptide betatide, which has demonstrated antimicrobial effects in multiple multi-resistant bacterial strains [9,10]. The concentration of betatide was 8 mg/L, which corresponds to half the MIC concentration.

The results that are summarized in Table 3 showed that all the compounds experience increased activity and lower MIC when they are combined with betatide. The activity trend

roughly followed that which was seen for the single agents with the *para*-bromo and the *para*-iodo derivatives 5 and 6 being most potent.

Table 3. Minimum inhibitory concentration (MIC) towards *S. aureus* as single agent and in combination with peptide betatide.

Comp.	4-Amino Group	Scaffold	Single Comp. MIC [mg/L]	Combination with Betatide MIC [mg/L]
				
				
				
1		A	64	8
2		A	16	8
4		A	16	4
5		A	8	1
6		A	8	2
7		A	16	4
19		B	8	2
21		C	32	4
Betatide	-	-	16	-

2.3.4. Structure-Activity Relationship

The SAR information that was gathered is shown in Figure 1. Crucial for activity is a phenolic group in *para* or *meta* position of the 6-aryl group. The other substitution patterns that were tested resulted in no activity.

Although some activity is retained when the heteroatom in the five membered ring is substituted for sulphur, the corresponding pyrrolopyrimidines were more active. For the 4-amino group, a single methyl group in R₃ switches activity on and off. Thus, R₂ should be a methyl and R₃ must be a hydrogen. Other alkyls as R₂ were not tested. For the R₁-substituents at the benzylamine there was a preference for *para*-substitution by bromine and iodine. Further studies on the variation of the R₁ group must be performed to verify if the increase in the activity is caused by the halogens or if it is purely a size effect.

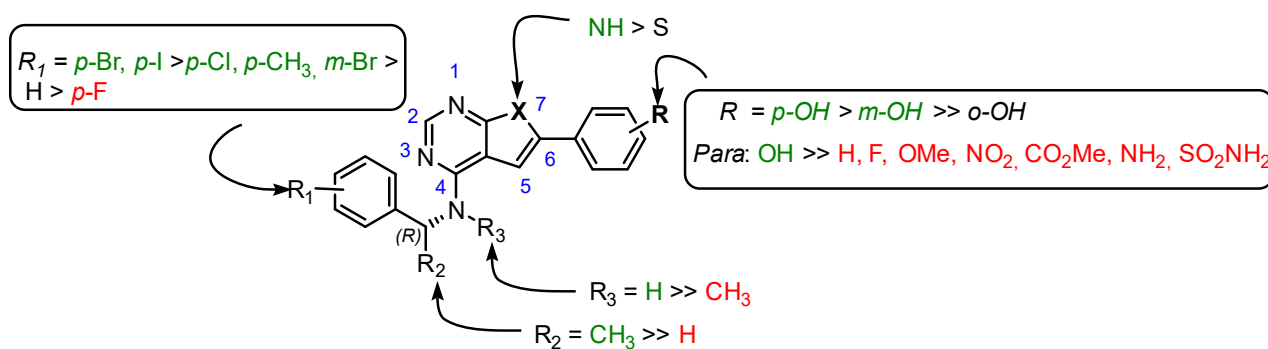


Figure 1. Structure-activity relationship that was identified for the inhibitors in this study. The green color denotes high activity, black medium, and red low.

2.4. Kinase Off-Targets and Mechanistic Studies

Based on the similarity of **5** with structures in our previous study [12], one could assume the bromo derivative **5** to be a TMPK inhibitor. Unfortunately, an assay towards *S. aureus* TMPK was not available. Instead, compound **5** was assayed towards the human and *E. coli* variant of TMPK, see Figure 2. Compound **5** had an IC_{50} of 5 μM towards *E. coli* TMPK and $>100 \mu\text{M}$ towards the human variant. Thus, even though the sequence similarity is not high (34% by Protein Blast), TMPK could be a target also in *S. aureus* as the folding (see Figure S41 in Supplementary Materials) and important residues in the catalytic domains: LID, *p*-loop, and the DRX motif are highly conserved [41,42].

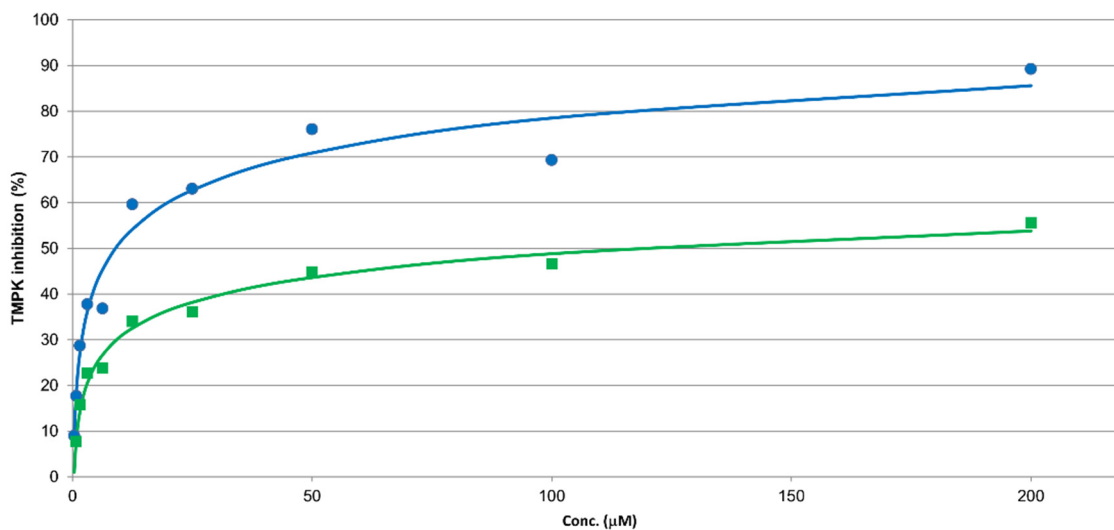


Figure 2. IC_{50} curves for inhibition of *E. coli* (blue circles) and human (green squares) TMPK for compound **5**.

As the starting point of this study was the EGFR inhibitor PKI-166 (**1**), there is an obvious risk of kinase off-target effects for the bromo derivative **5**. Therefore, we profiled **5** towards a panel of 50 human kinases. The most inhibited kinase was EGFR (91% inhibition at 500 nM test concentration), while very low inhibition was seen towards all the other kinases that were tested. This is shown in Figure 3. A follow up IC_{50} measurement towards EGFR showed PKI-166 (**1**) to have $IC_{50} < 1 \text{ nM}$, while **5** had an IC_{50} of 25 nM. Based on our previous experience [43,44], it is assumed that the EGFR inhibiting activity of **5** is too low to cause in vivo effects.

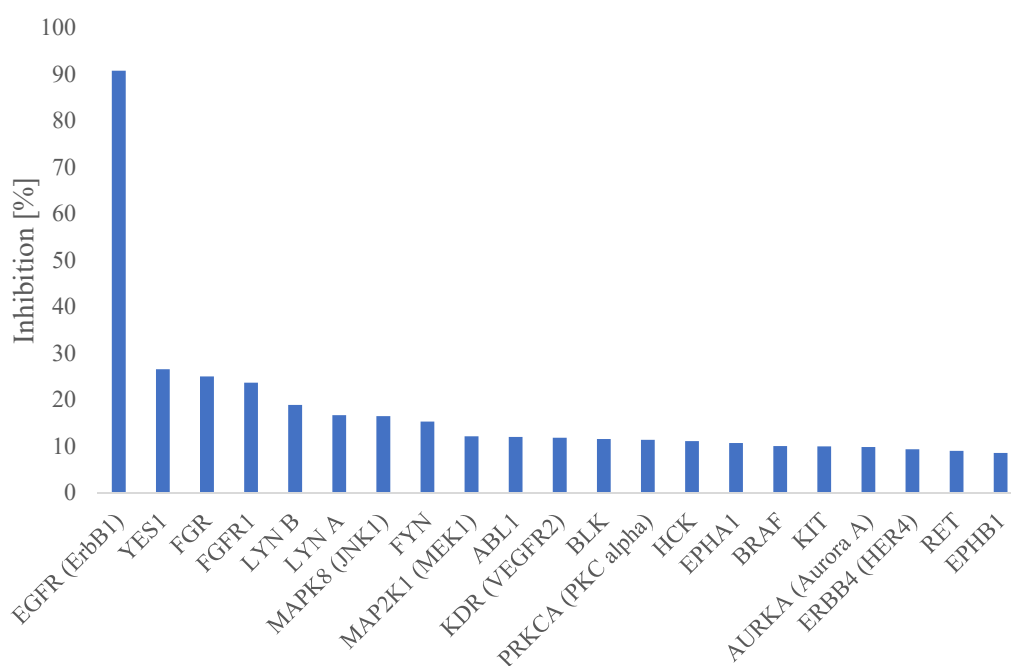


Figure 3. Inhibition profile for **5** against the 20 most inhibited human kinases, sorted by activity. The inhibitor concentration was 500 nM for all the kinases that were tested.

The enhanced pyrrolopyrimidine MIC when combined with betatide could be due to the enhanced uptake as betatide also affects the membrane via its cell penetrating peptide region [9]. In order to explore this further we combined compound **5** with commercial antibiotics targeting the membrane (cefotixin, methicillin, and only the cell penetrating part of betatide) or the bacterial translational machinery (gentamycin and clindamycin). We found a combinatory effect with some, but not all, of both types of antibiotics (data are not shown). This suggests that the combinatory effects between the fused pyrimidines and betatide are due to intracellular mechanisms and not an increased uptake of the compounds. Further studies to explore the molecular mechanisms behind the combinatory effects are ongoing.

3. Experimental Section

3.1. Chemicals and Materials

All the reagents and solvents used were purchased from Merck (Rahway, NJ, USA), VWR (Sugar Land, TX, USA) or Alpha Aesar (Ward Hill, MA, USA) and used without further purification. Compound **3** was previously prepared by Kaspersen et al. [45]. The reactions that were sensitive to moisture or oxygen were conducted under an N₂ atmosphere using oven-dried glassware and solvents that were dried over molecular sieves for 24 h or collected from an MBraun SPS-800 solvent purifier. For flash chromatography, different stationary phases were used: for normal phase, silica-gel (40–63 µm particle size) purchased from VWR, prepackaged cartridges (Biotage Sfär Silica D Duo 60 µm and Biotage Sfär Silica HC D, 20 µm, Biotage, Uppsala, Sweden, and Alumina, neutral, Brockmann I (58 Å pore size) that was purchased from Merck. For reversed phase flash chromatography prepackaged cartridges from Biotage (Biotage Sfär C18 D, 100 Å, 30 µm, 12 g) were used.

3.2. Analysis and Characterization

Accurate mass determination in positive and negative mode was performed on a “Synapt G2-S” Q-TOF instrument from WatersTM (Milford, MA, USA). The samples were ionized using an ASAP probe (APCI). No chromatographic separation was done prior to the mass analysis. The calculated exact mass and spectra processing was done by WatersTM Software (Masslynx V4.1 SCN871). NMR spectra were recorded using the Bruker DPX

400 MHz and 600 MHz Avance III HD NMR spectrometers. Chemical shifts (δ) are recorded in parts per million relative to TMS ($\delta_{\text{H}} = 0.00$, $\delta_{\text{C}} = 0.00$), CDCl_3 ($\delta_{\text{H}} = 7.26$, $\delta_{\text{C}} = 77.16$), or $\text{DMSO}-d_6$ ($\delta_{\text{H}} = 2.50$, $\delta_{\text{C}} = 39.52$), and coupling constants (J) are measured in hertz (Hz). Purity analyses: HPLC purity analyses were performed on an Agilent 1260 series instrument with an ACE Excel 5 C18 column (4.6 mm \times 150 mm, $d_{\text{p}} = 5 \mu\text{m}$) with a flow of 1 mL/min, UV monitoring at 320 nm, and with Agilent Chemstation as the software. Elution: 10 min linear gradient of MeCN/H₂O (35:65) to MeCN/H₂O (70:30) followed by 5 min linear gradient of MeCN/H₂O (70:30) to MeCN/H₂O (100:0). The enantiomeric excess of the intermediate **34** was controlled by HPLC using an Agilent 1100 series system detecting at 254 nm and using a Chiracel OD column (4.6 mm \times 250 mm, $d_{\text{p}} = 10 \mu\text{m}$), mobile phase: *n*-hexane/2-propanol, 87:13, flow rate 1.0 mL/min; $t_{\text{R}} = 8.15$ min, $t_{\text{S}} = 9.47$ min, $R_{\text{s}} = 1.7$.

3.3. Synthetic Protocols

3.3.1. Amination of Fused Pyrimidines (General Procedure A)

The following procedure is adapted from Kaspersen et al. [45]. The pyrrolo- or thienopyrimidine (100–200 mg) was flushed with N₂ three times and dissolved in degassed *n*-BuOH (1–2 mL). DIPEA (0–6 equiv.) and amine (3 equiv.) were then added, and the reaction was stirred under an N₂ atmosphere at an oil bath temperature of 140 °C for 18–24 h. The solution was then cooled to an ambient temperature and the solvent was removed in vacuo, facilitated by the addition of toluene. The resulting solid was suspended between EtOAc (25 mL) and H₂O (25 mL) and separated. The aqueous layer was extracted with EtOAc (3 \times 25 mL) and the combined organic layers were washed with brine (25 mL), dried over anhydrous Na₂SO₄, filtered, and concentrated in vacuo. The material was then purified by flash chromatography as described for each specific compound.

3.3.2. Regioselective Suzuki Cross-Coupling (General Procedure B)

To a mixture of (*R*) or (*S*)-*N*-(1-(4-bromophenyl)ethyl)-6-iodo-7-((2-(trimethylsilyl)ethoxy)methyl)-7*H*-pyrrolo [2,3-*d*] pyrimidin-4-amine (**34**) (100–300 mg), arylboronic acid (1 equiv.), Pd (dppf) Cl₂ (0.05 equiv.), and K₂CO₃ (3 equiv.) under N₂, degassed 1,4-dioxane (2 mL) and water (1 mL) were added. The mixture was stirred at 80 °C until full conversion as noted by TLC or ¹H NMR, before it was filtered through a celite pad which was rinsed with CH₂Cl₂ (4 \times 10 mL) and the mixture was concentrated to dryness under reduced pressure. The solids were dissolved in CH₂Cl₂ (20 mL) and water (20 mL) and separated. The aqueous phase was extracted with CH₂Cl₂ (3 \times 20 mL) before the combined organic phase was dried over Na₂SO₄, filtered, and concentrated in vacuo. The crude material was purified by flash chromatography as specified for each compound.

3.3.3. SEM-Deprotection (General Procedure C)

The following two-step procedure is adapted from Reiersølmoen et al. [46]. The SEM-protected pyrrolopyrimidine (50–100 mg) was flushed with N₂ three times and dissolved in CH₂Cl₂ and TFA (1–2 mL). The reaction was then stirred under an N₂ atmosphere at ambient temperature for 3–4 h. The TFA was then removed in vacuo, and co-evaporated twice with MeOH (3 \times 10 mL) to remove traces of TFA. The reaction mixture was then dissolved in 1,4-dioxane (5–10 mL) and sat. NaHCO₃ solution was added. This suspension was stirred overnight, before the solvent was removed in vacuo. The solid was then distributed between EtOAc (10–20 mL) and H₂O (10–20 mL) and separated. The aqueous layer was extracted with EtOAc (4 \times 10–20 mL) and the combined organic layers were washed with brine (10–20 mL), dried over anhydrous Na₂SO₄, filtered, and concentrated in vacuo. The solid was then purified as described in the specific experimental section.

3.4. Preparation of Compounds 1–21

3.4.1. (*R*)-4-(4-((1-Phenylethyl)amino)-7*H*-pyrrolo[2,3-*d*]pyrimidin-6-yl)phenol (**1**)

Compound **1** was prepared as described in General Procedure C, starting from **25** (43 mg, 92.7 μmol). Immobilization on celite and purification by gradient flash chromatog-

raphy (C18 silica, MeCN/H₂O, 1:9 to 3:2) resulted in 23 mg (70.8 μ mol, 76%) of the desired product as a white solid, mp. 226.6–228.4 °C (decomp.), $[\alpha]_D^{20} = -290$ (c 0.50, EtOH), HPLC purity: 99%, $t_R = 5.61$ min; TLC (H₂O/MeCN 3:2) $R_f = 0.30$; ¹H NMR (600 MHz, DMSO-*d*₆) δ : 11.82 (s, 1H), 9.61 (s, 1H), 8.02 (s, 1H), 7.68 (d, $J = 8.2$ Hz, 1H), 7.63–7.57 (m, 2H), 7.45–7.40 (m, 2H), 7.33–7.27 (m, 2H), 7.22–7.16 (m, 1H), 6.88 (d, $J = 2.2$ Hz, 1H), 6.85–6.80 (m, 2H), 5.49 (*p*, $J = 7.1$ Hz, 1H), 1.53 (d, $J = 7.0$ Hz, 3H); ¹³C NMR (151 MHz, DMSO-*d*₆) δ : 157.0, 154.7, 151.1, 145.6, 134.0, 128.1 (2C), 126.4, 126.05 (2C), 126.03 (2C), 123.0, 115.7 (2C), 103.9, 93.9, 48.7, 22.9; IR (neat, cm⁻¹): 3114 (O-H), 1596 (N-H), 1497 (Ar C-H), 699 (Ar C-H); HRMS (TOF ES+, *m/z*): calcd. for C₂₀H₁₉N₄O [M + H]⁺: 331.1559, found: 331.1565. This material was first reported by Traxler et al. [47].

3.4.2. (R)-4-(4-((1-(*p*-Tolyl)ethyl)amino)-7*H*-pyrrolo[2,3-*d*]pyrimidin-6-yl)phenol (2)

Compound **2** was prepared as described in General Procedure C, starting from **26** (102 mg, 0.215 mmol). The crude material was purified by preparative LC (Agilent Prep C-18 150 \times 21.2 mm, 5 μ m column, 20 mL/min flow, MeCN/H₂O, 30:70 to 70:30 (0–10 min linear gradient), followed by 70:30–100:0 (10–15 min linear gradient), 100 μ L injection, $\lambda = 320$ nm, $t_R = 8.139$ min), resulting in 14 mg (40.4 μ mol, 19%) of the desired product as a white solid, $[\alpha]_D^{20} = -266$ (c 0.50, EtOH), HPLC purity: 96%, $t_R = 6.49$ min. ¹H NMR (600 MHz, DMSO-*d*₆) δ : 11.80 (s, 1H), 9.60 (s, 1H), 8.01 (s, 1H), 7.62 (d, $J = 8.3$ Hz, 1H), 7.61–7.56 (m, 2H), 7.33–7.26 (m, 2H), 7.10 (m, 2H), 6.87 (d, $J = 2.2$ Hz, 1H), 6.85–6.79 (m, 2H), 5.44 (*p*, $J = 7.2$ Hz, 1H), 2.25 (s, 3H), 1.50 (d, $J = 7.0$ Hz, 3H); ¹³C NMR (151 MHz, DMSO-*d*₆) δ : 156.9, 154.3, 151.1, 142.6, 135.3, 134.0, 128.7 (2C), 126.02 (2C), 125.97 (2C), 123.0, 115.7 (2C), 103.7, 94.6, 48.4, 22.9, 20.6; IR (neat, cm⁻¹): 3136 (O-H), 1598 (N-H), 1498 (Ar C-H), 835 (Ar C-H); HRMS (TOF ES+, *m/z*): calcd. for C₂₁H₂₁N₄O [M + H]⁺: 345.1715, found: 345.1719.

3.4.3. (R)-4-(4-((1-(4-Chlorophenyl)ethyl)amino)-7*H*-pyrrolo[2,3-*d*]pyrimidin-6-yl)phenol (4)

Compound **4** was prepared as described in General Procedure C, starting from **27** (51 mg, 0.103 mmol). Extraction with EtOAc and H₂O resulted in 37 mg (0.101 mmol, 98%) of the desired product as a light-yellow solid, mp. 216.6 °C (decomp.), $[\alpha]_D^{20} = -352$ (c 0.50, EtOH), HPLC purity: 96%, $t_R = 7.81$ min. ¹H NMR (600 MHz, DMSO-*d*₆) δ : 11.84 (s, 1H), 9.62 (s, 1H), 8.01 (s, 1H), 7.72 (d, $J = 8.0$ Hz, 1H), 7.63–7.58 (m, 2H), 7.46–7.41 (m, 2H), 7.38–7.33 (m, 2H), 6.87 (d, $J = 2.2$ Hz, 1H), 6.86–6.80 (m, 2H), 5.45 (*p*, $J = 7.2$ Hz, 1H), 1.51 (d, $J = 7.0$ Hz, 3H); ¹³C NMR (151 MHz, DMSO-*d*₆) δ : 157.0, 151.1, 144.8, 134.2, 130.9, 128.1 (2C), 128.0 (2C), 126.1 (2C), 122.9, 115.7 (2C), 103.9, 93.9, 48.2, 22.8; IR (neat, cm⁻¹): 3129 (O-H), 1599 (N-H), 1495 (Ar C-H), 833 (Ar C-H); HRMS (TOF ES+, *m/z*): calcd. for C₂₀H₁₈N₄OCl [M+H]⁺ 365.1169, found: 365.1169.

3.4.4. (R)-4-(4-((1-(4-Bromophenyl)ethyl)amino)-7*H*-pyrrolo[2,3-*d*]pyrimidin-6-yl)phenol (5) from **28**

Compound **5** was prepared as described in General Procedure C, starting from **28** (42 mg, 0.078 mmol). The crude product was dissolved in MeOH (3 mL) and purified by gradient flash chromatography (C18 silica, MeOH/H₂O, 1:1 to 9:1). TLC (MeOH/H₂O, 9:1) $R_f = 0.48$. This afforded 22 mg (0.054 mmol, 69%) as a white solid; HPLC purity: 96%, $t_R = 7.37$ min; $[\alpha]_D^{20} = -352.0$ (1.00, EtOH (96%)); ¹H NMR (600 MHz, DMSO-*d*₆) δ : 11.81 (s, 1H), 8.00 (s, 1H), 7.70 (d, $J = 8.0$ Hz, 1H), 7.59–7.57 (m, 2H), 7.51–7.48 (m, 2H), 7.39–7.38 (m, 2H), 6.84 (s, 1H), 6.81–6.79 (m, 2H), 5.43 (*p*, $J = 7.2$ Hz, 1H), 1.51 (d, $J = 7.0$ Hz, 3H), OH-signal not seen; ¹³C NMR (150 MHz, DMSO-*d*₆) δ : 158.2, 154.5, 151.2, 150.9, 145.3, 134.5, 131.0 (2C), 128.3 (2C), 126.0 (2C), 122.0, 119.3, 116.0 (2C), 103.9, 93.5, 48.3, 22.8; IR (neat, cm⁻¹): 3328 (N-H), 3122 (O-H), 1596 (N-H), 834 (Ar C-H); HRMS (ASAP-TOF, *m/z*): calcd. for C₂₀H₁₈N₄O⁷⁹Br, 409.0664 [M + H]⁺, found 409.0670.

3.4.5. (*R*)-4-(4-((1-(4-Bromophenyl)ethyl)amino)-7*H*-pyrrolo[2,3-*d*]pyrimidin-6-yl)phenol (**5**) from **35**

The following procedure is adapted from Kaspersen et al. [45]. Compound **35** (38 mg, 69.4 μmol) was dissolved in CH_2Cl_2 (1 mL) and stirred at 0 °C under an N_2 atmosphere. BBr_3 (1 M, 700 μL) was added dropwise over 1 hour, and the reaction was stirred for a further 1.5 h at 22 °C. The reaction was then cooled to 0 °C and quenched by the addition of H_2O (4 mL) and saturated NaHCO_3 solution (1 mL). The pH was adjusted to 4 with HCl (2 M) and saturated NaHCO_3 solution. The solution was then distributed between EtOAc (25 mL) and H_2O (25 mL) and separated. The aqueous phase was extracted with EtOAc (3 \times 25 mL) and the combined organic layers were washed with brine (25 mL), dried over anhydrous Na_2SO_4 , filtered, and concentrated in vacuo. The resulting crude product was dissolved in 1,4-dioxane (10 mL) and saturated NaHCO_3 solution (1 mL) was added. The solution was stirred under an N_2 atmosphere overnight, before it was concentrated in vacuo and suspended in H_2O (25 mL) and EtOAc (25 mL). The pH in the aqueous phase was adjusted to 5 with HCl (2 M) and saturated NaHCO_3 solution. The phases were separated, and the aqueous layer was extracted with EtOAc (3 \times 25 mL). The combined organic phases were washed with brine, dried over Na_2SO_4 , filtered, and concentrated in vacuo. The resulting crude was immobilized on Celite and purified by flash chromatography (C18-silica, MeCN/ H_2O cont. 0.1% NEt_3 in H_2O , 3:2, $R_f = 0.29$), resulting in 12 mg (2.86 μmol , 41%) of the desired product as a light-yellow solid. The ^1H NMR spectroscopic data confirmed with that which is reported above [45].

3.4.6. (*R*)-4-(4-((1-(4-Iodophenyl)ethyl)amino)-7*H*-pyrrolo[2,3-*d*]pyrimidin-6-yl)phenol (**6**)

Compound **6** was prepared as described in General Procedure C, starting from **29** (51 mg, 86.1 μmol). Immobilization on celite and purification by gradient flash chromatography (C18 silica, MeCN/ H_2O , 1:9 to 3:2) resulted in 22 mg (48.4 μmol , 56%) of the desired product as a light-yellow solid, mp. 254.9–256.0 °C (decomp.), TLC (MeCN/ H_2O 3:2) $R_f = 0.24$; $[\alpha]_D^{20} = -356$ (c 0.50, EtOH), HPLC purity: 97%, $t_R = 7.85$ min. ^1H NMR (600 MHz, DMSO- d_6) δ : 11.84 (s, 1H), 9.62 (s, 1H), 8.00 (s, 1H), 7.70 (d, $J = 8.0$ Hz, 1H), 7.68–7.63 (m, 2H), 7.63–7.57 (m, 2H), 7.26–7.21 (m, 2H), 6.86 (d, $J = 2.1$ Hz, 1H), 6.85–6.76 (m, 2H), 5.40 (*p*, $J = 7.2$ Hz, 1H), 1.50 (d, $J = 6.9$ Hz, 3H); ^{13}C NMR (151 MHz, DMSO- d_6) δ : 157.0, 151.3, 151.1, 145.7, 136.9 (2C), 134.2, 128.5 (2C), 126.1 (2C), 122.9, 115.7 (2C), 103.9, 93.9, 92.0, 48.4, 22.7; IR (neat, cm^{-1}): 3139 (O-H), 1598 (N-H), 1498 (Ar C-H), 834 (Ar C-H); HRMS (TOF ES+, m/z): calcd. for $\text{C}_{20}\text{H}_{18}\text{N}_4\text{OI}$ [$\text{M} + \text{H}$] $^+$: 457.0525, found: 457.0534.

3.4.7. (*R*)-4-(4-((1-(3-Bromophenyl)ethyl)amino)-7*H*-pyrrolo[2,3-*d*]pyrimidin-6-yl)phenol (**7**)

Compound **7** was prepared as described in General Procedure C, starting from **30** (103 mg, 0.190 mmol). Immobilization on celite and purification by gradient flash chromatography (silica, EtOAc/*n*-pentane 0:1 to 1:1) resulted in 49 mg (0.199 mmol, 63%) of the desired product as an off-white solid, decomp. at 237.5–240.1 °C, TLC (EtOAc/*n*-pentane 1:1) $R_f = 0.39$; $[\alpha]_D^{20} = -228$ (c 0.5, EtOH), HPLC purity: 98%, $t_R = 7.24$ min. ^1H NMR (600 MHz, DMSO- d_6) δ : 11.86 (s, 1H), 9.62 (s, 1H), 8.02 (s, 1H), 7.74 (d, $J = 8.1$ Hz, 1H), 7.64–7.58 (m, 3H), 7.45–7.40 (m, 1H), 7.40–7.37 (m, 1H), 7.27 (t, $J = 7.8$ Hz, 1H), 6.86 (d, $J = 2.2$ Hz, 1H), 6.86–6.80 (m, 2H), 5.48–5.43 (m, 1H), 1.51 (d, $J = 7.0$ Hz, 3H); ^{13}C NMR (151 MHz, DMSO- d_6) δ : 157.0, 154.5, 151.1, 148.8, 134.3, 130.5, 129.3, 128.7, 126.1, 125.3, 122.9, 121.6, 115.7, 103.9, 93.8, 48.4, 22.9; IR (neat, cm^{-1}): 3111 (O-H), 1596 (N-H), 1498 (Ar C-H), 521 (C-Br); HRMS (TOF ES+, m/z): calcd. for $\text{C}_{20}\text{H}_{18}\text{N}_4\text{O}^{79}\text{Br}$ [$\text{M} + \text{H}$] $^+$: 409.0664, found: 409.0667.

3.4.8. 4-(4-((4-Bromobenzyl)amino)-7*H*-pyrrolo[2,3-*d*]pyrimidin-6-yl)phenol (**8**)

Compound **8** was prepared as described in General Procedure C starting from **31** (111 mg, 0.211 mmol). Immobilization on celite and purification by gradient flash chromatography (C18 silica, MeCN/ H_2O , 1:9 to 1:0) gave the desired product in a yield of 11 mg (28.5 μmol , 13%) as an off-white solid, TLC (MeCN/ H_2O 3:2) $R_f = 0.33$; HPLC purity:

96%, $t_R = 6.65$ min. ^1H NMR (600 MHz, $\text{DMSO-}d_6$) δ : 11.87 (s, 1H), 9.61 (s, 1H), 8.07 (s, 1H), 7.94 (t, $J = 6.1$ Hz, 1H), 7.60–7.58 (m, 2H), 7.52–7.48 (m, 2H), 7.32–7.30 (m, 2H), 6.84–6.81 (m, 2H), 6.76 (d, $J = 2.2$ Hz, 1H), 4.68 (d, $J = 6.1$ Hz, 2H); ^{13}C NMR (151 MHz, $\text{DMSO-}d_6$) δ : 157.0, 155.3, 151.2, 151.2, 140.0, 134.3, 131.1 (2C), 129.4 (2C), 126.1 (2C), 122.9, 119.5, 115.7 (2C), 103.9, 93.6, 42.6; IR (neat, cm^{-1}): 3421 (N-H), 3109 (O-H), 1599 (N-H), 1500 (Ar C-H), 800 (Ar C-H); HRMS (TOF ES+, m/z): calcd. for $\text{C}_{19}\text{H}_{16}\text{N}_4\text{O}^{79}\text{Br}$ $[\text{M} + \text{H}]^+$ 395.0507, found: 395.0504.

3.4.9. (S)-4-(4-((1-(4-Bromophenyl)ethyl)amino)-7H-pyrrolo[2,3-d]pyrimidin-6-yl)phenol (9)

Compound **9** was prepared as described in General Procedure C starting from **32** (98.8 mg, 0.183 mmol). Immobilization on celite and purification by gradient flash chromatography (C18 silica, MeCN/ H_2O , 1:9 to 1:0). This gave 49 mg (48.7 mg, 0.199 mmol, 65%) of a white solid, mp. 253.1–254.5 °C (decomp.); TLC (MeOH/ H_2O , 9:1) $R_f = 0.48$; ^1H NMR (600 MHz, $\text{DMSO-}d_6$) δ : 11.85 (s, 1H), 9.63 (s, 1H), 8.02 (s, 1H), 7.72 (d, $J = 8.0$ Hz, 1H), 7.61 (d, $J = 8.1$ Hz, 2H), 7.49 (d, $J = 8.5$ Hz, 2H), 7.38 (d, $J = 8.5$ Hz, 2H), 6.87 (s, 1H), 6.84 (d, $J = 8.0$ Hz, 2H), 5.43 (p, $J = 7.2$ Hz, 1H), 1.51 (d, $J = 7.0$ Hz, 3H); ^{13}C NMR (151 MHz, $\text{DMSO-}d_6$) δ : 157.0, 154.6, 151.3, 151.1, 145.2, 134.2, 131.0 (2C), 128.4 (2C), 126.1 (2C), 122.9, 119.3, 115.7 (2C), 103.9, 93.9, 48.6, 22.8; IR (neat, cm^{-1}): 2975 (C-H), 1547 (N-H), 834 (Ar C-H), 548 (C-Br); HRMS (TOF ES+, m/z): calcd. for $\text{C}_{20}\text{H}_{18}\text{N}_4\text{O}^{79}\text{Br}$ $[\text{M} + \text{H}]^+$: 409.0664, found: 409.0664. The ^1H NMR shifts are found at higher field than that reported for the corresponding HBr-salt [48].

3.4.10. (R)-4-(4-((1-(4-Bromophenyl)ethyl)(methyl)amino)-7H-pyrrolo[2,3-d]pyrimidin-6-yl)phenol (10)

Compound **10** was prepared as described in General Procedure C starting from **33** (52 mg, 93.9 μmol). Immobilization on celite and purification by gradient flash chromatography (silica, MeOH/ CH_2Cl_2 , 0:100 to 5:95) yielded a yellow solid, which after a wash with toluene (5 mL) resulted in the desired product with a yield of 59% (18.8 mg, 44.4 μmol) as an off-white solid, TLC (MeOH/ CH_2Cl_2 3:2) $R_f = 0.24$; $[\alpha]_D^{20} = -10.0$ (c 0.50, DMF); HPLC purity: 98.5%, $t_R = 9.57$ min; ^1H NMR (600 MHz, $\text{DMSO-}d_6$) δ : 12.00 (s, 1H), 9.58 (s, 1H), 8.13 (s, 1H), 7.72–7.65 (m, 2H), 7.58–7.49 (m, 2H), 7.32–7.24 (m, 2H), 6.88 (d, $J = 2.2$ Hz, 1H), 6.84–6.76 (m, 2H), 6.39 (s, 1H), 3.06 (s, 3H), 1.58 (d, $J = 7.0$ Hz, 3H); ^{13}C NMR (151 MHz, $\text{DMSO-}d_6$) δ : 157.0, 156.2, 152.8, 150.5, 141.3, 133.9, 131.3 (2C), 129.2 (2C), 126.3 (2C), 122.6, 120.0, 115.6 (2C), 103.6, 96.8, 51.9, 40.1, 31.5, 16.2; IR (neat, cm^{-1}): 3115 (O-H), 1568 (N-H), 1490 (Ar C-H), 827 (Ar C-H); HRMS (TOF ES+, m/z): calcd. For $\text{C}_{21}\text{H}_{20}\text{N}_4\text{O}^{79}\text{Br}$ $[\text{M} + \text{H}]^+$: 423.0820, found: 423.0826.

3.4.11. (S)-N-(1-(4-Bromophenyl)ethyl)-6-(4-methoxyphenyl)-7H-pyrrolo[2,3-d]pyrimidin-4-amine (11)

Compound **11** was prepared as described in General Procedure C starting from **35** (120 mg, 0.217 mmol). The crude product was purified twice by C18 silica flash chromatography (first MeOH/EtOAc, 3:1, then: acetone/ H_2O , 1:1, TLC (C18 silica acetone/ H_2O , 1:1) $R_f = 0.68$). This gave 33 mg (0.078 mmol, 36%) as an off-white solid; HPLC purity: 98%, $t_R = 9.86$ min; $[\alpha]_D^{20} = +288.2$ (1.00, EtOH (100%)); ^1H NMR (600 MHz, $\text{DMSO-}d_6$) δ : 11.932–11.929 (m, 1H), 8.02 (s, 1H), 7.76 (d, 1H, $J = 8.1$ Hz), 7.73–7.71 (m, 2H), 7.50–7.48 (m, 2H), 7.39–7.37 (m, 2H), 7.03–7.01 (m, 2H), 6.94–6.93 (br d, 1H, $J = 1.6$ Hz), 5.43 (quint., 1H, $J = 7.2$ Hz), 3.80 (br s, 3H), 1.51 (d, 3H, $J = 7.0$ Hz); ^1H NMR is in accordance with that reported at 400 MHz [48].

3.4.12. (R)-N-(1-(4-Bromophenyl)ethyl)-6-phenyl-7H-pyrrolo[2,3-d]pyrimidin-4-amine (12)

Compound **12** was prepared as described in General Procedure C starting from **36** (63 mg, 0.120 mmol). The crude product was purified twice by C18 silica gradient flash chromatography (first: acetone/MeOH, 0:100 to 1:4 acetone/MeOH, then: MeOH/ H_2O , 1:1 to 9:1. TLC (C-18 silica, acetone/MeOH, 1:4) $R_f = 0.50$). This gave 32 mg (0.082 mmol, 68%)

as a white solid; HPLC purity >99% $t_R = 10.03$ min; $[\alpha]_D^{20} = -369.0$ (1.00, EtOH abs); ^1H NMR (600 MHz, DMSO- d_6) δ : 12.05 (s, 1H), 8.05 (s, 1H), 7.84 (d, $J = 7.9$ Hz, 1H), 7.80–7.78 (m, 2H), 7.51–7.48 (m, 2H), 7.46–7.43 (m, 2H), 7.39–7.37 (m, 2H), 7.31–7.28 (m, 1H), 7.09 (d, $J = 1.6$ Hz, 1H), 5.44 (quint., $J = 7.4$ Hz, 1H), 1.52 (d, $J = 7.1$ Hz, 3H); ^{13}C NMR (150 MHz, DMSO- d_6) δ : 154.9, 151.7, 151.6, 145.1, 133.5, 131.7, 131.0 (2C), 129.0 (2C), 128.3 (2C), 127.3, 124.5 (2C), 119.4, 103.9, 96.0, 48.3, 22.7; IR (neat, cm^{-1}): 3415 (N-H), 3114 (C-H), 1595 (N-H), 1475 (Ar C-H), 751 (C-H); HRMS (ASAP-TOF, m/z): calcd. for $\text{C}_{20}\text{H}_{18}\text{N}_4^{79}\text{Br}$, 393.0715 [$\text{M} + \text{H}$] $^+$, found 393.0715.

3.4.13. (R)-N-(1-(4-Bromophenyl)ethyl)-6-(4-fluorophenyl)-7H-pyrrolo[2,3-d]pyrimidin-4-amine (13)

Compound **13** was prepared as described in General Procedure C starting from **37** (63 mg, 0.116 mmol). The crude product was purified by gradient flash chromatography (C18 silica, MeOH/H₂O, 1:1 to 9:1). TLC (MeOH/H₂O, 9:1, $R_f = 0.20$). This gave 37 mg (0.090 mmol, 78%) as a white solid; HPLC purity: 99%, $t_R = 10.310$ min; $[\alpha]_D^{20} = -317.0$ (1.00, EtOH abs); ^1H NMR (600 MHz, CDCl₃) δ : 12.82 (s, 1H), 8.31 (s, 1H), 7.75–7.69 (m, 2H), 7.50–7.45 (m, 2H), 7.35–7.30 (m, 2H), 7.21–7.14 (m, 2H), 6.53 (d, $J = 1.9$ Hz, 1H), 5.52 (*p*, $J = 7.0$ Hz, 1H), 5.28 (s, 1H), 1.66 (d, $J = 6.9$ Hz, 3H); ^{13}C NMR (150 MHz, CDCl₃) δ : 162.7 (d, $J = 247.6$ Hz), 155.5, 152.0, 151.6, 143.3, 135.3, 131.9 (2C), 128.5 (d, $J = 3.2$ Hz), 128.0 (2C), 127.3 (d, $J = 8.8$ Hz, 2C), 121.2, 116.3 (d, $J = 22.0$ Hz, 2C), 104.6, 94.5, 49.9, 23.0; ^{19}F NMR (376 MHz, CDCl₃, C₆F₆) δ : -116.3 (s); IR (neat, cm^{-1}): 3428 (N-H), 2976 (C-H), 1596 (N-H), 1496 (Ar C-H), 834 (Ar C-H); HRMS (ASAP-TOF, m/z): calcd. for $\text{C}_{20}\text{H}_{17}\text{N}_4\text{F}^{79}\text{Br}$, 411.0621 [$\text{M} + \text{H}$] $^+$, found 411.0621.

3.4.14. (R)-N-(1-(4-Bromophenyl)ethyl)-6-(4-nitrophenyl)-7H-pyrrolo [2,3-d]pyrimidin-4-amine (14)

Compound **14** was prepared as described in General Procedure C starting from **38** (185 mg, 0.325 mmol). The crude product was dissolved in DMF (2 mL) at 75 °C and water was added dropwise until saturation, which produced precipitation upon cooling. This afforded 73 mg (0.167 mmol, 51%) of a yellow-orange solid; HPLC purity: 96%, $t_R = 10.37$ min; $[\alpha]_D^{20} = -635.0$ (1.00, DMSO); ^1H NMR (600 MHz, DMSO- d_6) δ : 12.37 (s, 1H), 8.32–8.30 (m, 2H), 8.11 (s, 1H), 8.07 (d, $J = 7.9$ Hz, 1H), 8.03–8.00 (m, 2H), 7.51–7.49 (m, 2H), 7.39–7.37 (m, 3H), 5.45 (*p*, $J = 7.1$ Hz, 1H), 1.53 (d, $J = 7.0$ Hz, 3H); ^{13}C NMR (150 MHz, DMSO- d_6) δ : 155.3, 153.0, 152.3, 145.7, 144.8, 138.0, 131.2, 131.1 (2C), 128.3 (2C), 125.0 (2C), 124.5 (2C), 119.5, 104.2, 100.1, 48.4, 22.6; IR (neat, cm^{-1}): 3407 (N-H), 2973 (C-H), 1601 (N-H), 1536 (N-O), 1489 (Ar C-H), 828 (Ar C-H); HRMS (ASAP-TOF, m/z): calcd. for $\text{C}_{20}\text{H}_{17}\text{N}_5\text{O}_2^{79}\text{Br}$, 438.0566 [$\text{M} + \text{H}$] $^+$, found 438.0563.

3.4.15. (R)-6-(4-Aminophenyl)-N-(1-(4-bromophenyl)ethyl)-7H-pyrrolo[2,3-d]pyrimidin-4-amine (15)

To a mixture the nitro derivative **14** (40 mg, 0.091 mmol), NH₄Cl (44 mg, 0.823 mmol) and Fe-powder (15 mg, 0.276 mmol) under a N₂ atmosphere, water (0.9 mL), and EtOH (96%, 2.1 mL) were added. The mixture was stirred at 78 °C for 5 hours before full conversion was observed by TLC. The mixture was filtered through a celite pad, which was washed with EtOAc (75 mL) and MeOH (100 mL), and the solution was dried in vacuo. The solids were added to water (20 mL) and EtOAc (50 mL), and the aqueous layer was adjusted to pH 9 with NaHCO₃ before the layers were separated, and the aqueous layer was extracted with additional EtOAc (3 × 20 mL). The combined organic phase was dried over Na₂SO₄, filtered, and concentrated in vacuo. The crude product was purified by gradient flash chromatography (C18 silica, MeOH/H₂O, 1:1 to 9:1). TLC (MeOH/H₂O, 9:1) $R_f = 0.39$. This afforded 17 mg (0.042 mmol, 45%) as an off-white solid; HPLC purity: 96%, $t_R = 7.34$ min; $[\alpha]_D^{20} = -315$ (1.00, acetone); ^1H NMR (600 MHz, DMSO- d_6) δ : 11.71 (br s, 1H), 7.98 (s, 1H), 7.66 (d, $J = 8.1$ Hz, 1H), 7.50–7.45 (m, 4H), 7.38–7.37 (m, 2H), 6.76 (d, $J = 2.1$ Hz, 1H), 6.62–6.60 (m, 2H), 5.42 (*p*, $J = 7.2$ Hz, 1H), 1.50 (d, $J = 7.0$ Hz, 3H) (NH₂-signal not observed); ^{13}C NMR (150 MHz, DMSO- d_6) δ : 154.2, 151.1, 150.5, 148.4, 145.3, 135.1, 131.0

(2C), 128.3 (2C), 125.7 (2C), 119.4, 119.3, 114.0 (2C), 104.0, 92.5, 48.3, 22.8; IR (neat, cm^{-1}): 3342 (N-H), 3214 (N-H), 2923 (C-H), 1594 (N-H), 1476 (Ar C-H), 825 (Ar C-H); HRMS (ASAP-TOF, m/z): calcd. for $\text{C}_{20}\text{H}_{19}\text{N}_5^{79}\text{Br}$, 408.0824 $[\text{M} + \text{H}]^+$, found 408.0829.

3.4.16. Methyl (R)-4-(4-((1-(4-bromophenyl)ethyl)amino)-7H-pyrrolo[2,3-d]pyrimidin-6-yl)benzoate (16)

Compound **16** was prepared as described in General Procedure C starting from **39** (74 mg, 0.127 mmol). The crude product was suspended in acetone (3 mL) and centrifuged at 4400 rpm for 10 min before the supernatant was removed. This gave 31 mg (0.069 mmol, 54%) as a white powder; HPLC purity: 99%, $t_R = 10.03$ min; $[\alpha]_D^{20} = -467.0$ (c 1.00, DMSO); ^1H NMR (600 MHz, $\text{DMSO}-d_6$) δ : 12.23 (d, $J = 2.2$ Hz, 1H), 8.08 (s, 1H), 8.03–8.01 (m, 2H), 7.97 (d, $J = 8.0$ Hz, 1H), 7.93–7.91 (m, 2H), 7.51–7.49 (m, 2H), 7.39–7.37 (m, 2H), 7.28 (d, $J = 2.1$ Hz, 1H), 5.45 (p, $J = 7.2$ Hz, 1H), 3.87 (s, 3H), 1.52 (d, $J = 7.0$ Hz, 3H); ^{13}C NMR (150 MHz, $\text{DMSO}-d_6$) δ : 165.9, 155.2, 152.5, 152.0, 144.9, 136.2, 132.2, 131.1 (2C), 129.9 (2C), 128.3 (2C), 127.7, 124.4 (2C), 119.4, 104.0, 98.4, 52.1, 48.4, 22.7; IR (neat, cm^{-1}): 3369 (N-H), 2969, 2949 (C-H), 1696 (C=O), 1597 (N-H), 1475 (Ar C-H), 823 (Ar C-H), 602 (C-Br); HRMS (ASAP-TOF, m/z): calcd. for $\text{C}_{22}\text{H}_{20}\text{N}_4\text{O}_2^{79}\text{Br}$, 451.0770 $[\text{M} + \text{H}]^+$, found 451.0770.

3.4.17. (R)-4-(4-((1-(4-Bromophenyl)ethyl)amino)-7H-pyrrolo[2,3-d]pyrimidin-6-yl)benzene-sulfonamide (17)

Compound **17** was prepared as described in General Procedure C starting from **40** (122 mg, 0.202 mmol). The crude material was purified by gradient flash chromatography (C18 silica, acetone/ H_2O , 0:100 to 1:1). TLC (acetone/ H_2O , 1:1) $R_f = 0.25$. This afforded 67 mg (0.142 mmol, 70%) as a white powder; HPLC purity: 96%, $t_R = 6.875$ min; $[\alpha]_D^{20} = -367$ (1.00, acetone); ^1H NMR (600 MHz, $\text{DMSO}-d_6$) δ : 12.22 (d, 1H, $J = 2.2$ Hz), 8.09 (s, 1H), 7.98 (d, 1H, $J = 8.0$ Hz), 7.96–7.94 (m, 2H), 7.89–7.86 (m, 2H), 7.52–7.49 (m, 2H), 7.40–7.37 (m, 4H), 7.25 (d, 1H, $J = 2.0$ Hz), 5.45 (quint., 1H, $J = 7.2$ Hz), 1.53 (d, 3H, $J = 7.0$ Hz); ^{13}C NMR (150 MHz, $\text{DMSO}-d_6$) δ : 155.2, 152.4, 151.9, 145.0, 142.2, 134.8, 132.0, 131.1 (2C), 128.3 (2C), 126.4 (2C), 124.6 (2C), 119.4, 104.0, 98.2, 48.4, 22.7; IR (neat, cm^{-1}): 3376 (N-H), 2923 (C-H), 1593 (N-H), 1477 (Ar C-H), 1331 (S=O), 827 (Ar C-H), 621 (C-Br); HRMS (ASAP-TOF, m/z): calcd. for $\text{C}_{20}\text{H}_{19}\text{N}_5\text{O}_2\text{S}^{79}\text{Br}$, 472.0443 $[\text{M} + \text{H}]^+$, found 472.0444.

3.4.18. (R)-2-(4-((1-(4-Bromophenyl)ethyl)amino)-7H-pyrrolo[2,3-d]pyrimidin-6-yl)phenol (18)

Compound **18** was prepared as described in General Procedure C starting from **41** (48 mg, 0.089 mmol). The crude product was purified by gradient flash chromatography (C18 silica, acetone/ H_2O , 1:3 to 4:1). TLC (C18 silica, acetone/ H_2O , 4:1) $R_f = 0.77$. This afforded 24 mg (0.059 mmol, 66%) of a white powder; HPLC purity: 97%, $t_R = 8.43$ min; $[\alpha]_D^{20} = -367.0$ (1.00, EtOH); ^1H NMR (600 MHz, $\text{DMSO}-d_6$) δ : 11.58 (br s, 1H), 10.06 (br s, 1H), 8.02 (s, 1H), 7.87 (d, $J = 8.0$ Hz, 1H), 7.71 (dd, $J = 7.8, 1.7$ Hz, 1H), 7.50–7.47 (m, 2H), 7.39–7.37 (m, 2H), 7.28 (s, 1H), 7.11 (ddd, $J = 8.1, 7.2, 1.6$ Hz, 1H), 6.98 (dd, $J = 8.2, 1.2$ Hz, 1H), 6.87 (td, $J = 7.5, 1.2$ Hz, 1H), 5.45 (quint., $J = 7.2$ Hz, 1H), 1.51 (d, $J = 7.1$ Hz, 3H); ^{13}C NMR (150 MHz, $\text{DMSO}-d_6$) δ : 154.8, 154.4, 151.3, 150.6, 145.3, 131.0 (2C), 130.7, 128.4 (2C), 127.9, 126.9, 119.3 (2C)*, 118.5, 116.3, 103.7, 99.4, 48.3, 22.6, *2 overlapping signals revealed by HMBC; IR (neat, cm^{-1}): 3404 (N-H), 3046 (O-H), 2969 (C-H), 1596 (N-H), 1470 (Ar C-H), 822 (Ar C-H), 582 (C-Br); HRMS (ASAP-TOF, m/z): calcd. for $\text{C}_{20}\text{H}_{18}\text{N}_4\text{O}^{79}\text{Br}$, 409.0664 $[\text{M} + \text{H}]^+$, found 409.0665.

3.4.19. (R)-3-(4-((1-(4-Bromophenyl)ethyl)amino)-7H-pyrrolo[2,3-d]pyrimidin-6-yl)phenol (19)

Compound **19** was prepared as described in General Procedure C starting from **42** (47 mg, 0.087 mmol). The crude product was purified by gradient flash chromatography (C18 silica, acetone/ H_2O , 1:1 to 2:1). TLC (silica-gel, acetone/ n -pentane 1:2) $R_f = 0.24$. This gave 28 mg (0.068, 78%) as a white solid; HPLC purity: 97%, $t_R = 7.65$ min; $[\alpha]_D^{20} = -296.0$

(c 1.00, EtOH); ^1H NMR (600MHz, DMSO- d_6) δ : 11.96 (br d, $J = 2.3$ Hz, 1H), 9.54 (s, 1H), 8.04 (s, 1H), 7.82 (d, $J = 8.0$ Hz, 1H), 7.50–7.48 (m, 2H), 7.39–7.37 (m, 2H), 7.23–7.21 (m, 2H), 7.164–7.157 (m, 1H), 7.00 (br d, $J = 2.2$ Hz 1H), 6.72–6.70 (m, 1H), 5.44 (quint., $J = 7.2$ Hz, 1H), 1.52 (d, $J = 7.0$ Hz, 3H); ^{13}C NMR (150 MHz, DMSO- d_6) δ : 157.7, 154.9, 151.6, 151.4, 145.1, 133.7, 133.0, 131.0 (2C), 129.9, 128.3 (2C), 119.3, 115.5, 114.5, 111.5, 95.9, 48.3, 30.7, 22.7; IR (neat, cm^{-1}): 3119 (O-H), 2965 (C-H), 1597 (N-H), 1475 (Ar C-H), 822 (Ar C-H), 687 (C-Br); HRMS (ASAP-TOF, m/z): calcd. for $\text{C}_{20}\text{H}_{18}\text{N}_4\text{O}^{79}\text{Br}$, 409.0664 [M + H] $^+$, found 409.0670.

3.4.20. (*R*)-*N*-(1-(4-Bromophenyl)ethyl)-6-(4-methoxyphenyl)thieno [2,3-*d*] pyrimidin-4-amine (**20**)

4-Chloro-6-(4-methoxyphenyl)thieno [2,3-*d*] pyrimidine (**44**) (228 mg, 0.823 mmol) and (*R*)-1-(4-bromophenyl)ethan-1-amine (365 μL , 2.50 mmol) were reacted as described in General Procedure A. The resulting crude material was purified by gradient flash chromatography (silica, EtOAc/*n*-pentane, 0:1 to 1:1), resulting in 187 mg (0.424 mmol, 52%) of the desired product as a yellow solid, mp. 107.1–109.4 $^\circ\text{C}$, TLC (EtOAc/*n*-pentane 4:1) $R_f = 0.29$; $[\alpha]_D^{20} = -416$ (c 0.50, EtOH), HPLC purity >99%, $t_R = 13.93$ min. ^1H NMR (600 MHz, DMSO- d_6) δ : 8.25 (s, 1H), 8.18 (d, $J = 7.7$ Hz, 1H), 8.02 (s, 1H), 7.66–7.60 (m, 2H), 7.54–7.48 (m, 2H), 7.41–7.35 (m, 2H), 7.11–7.05 (m, 2H), 5.45 (t, $J = 7.2$ Hz, 1H), 3.82 (s, 3H), 1.55 (d, $J = 7.0$ Hz, 3H). ^{13}C NMR (151 MHz, DMSO- d_6) δ : 164.7, 159.6, 155.5, 153.5, 144.2, 138.4, 131.2 (2C), 128.3 (2C), 127.0 (2C), 125.8, 119.6, 117.6, 114.8 (2C), 113.8, 55.3, 48.7, 22.4; IR (neat, cm^{-1}): 3297 (N-H), 1607 (N-H), 1523 (Ar C-H), 825 (Ar C-H); HRMS (TOF ES+, m/z): calcd. for $\text{C}_{21}\text{H}_{19}\text{BrN}_3\text{OS}$ [M + H] $^+$: 440.0432, found: 440.0436.

3.4.21. (*R*)-4-(4-((1-(4-Bromophenyl)ethyl)amino)thieno[2,3-*d*]pyrimidin-6-yl)phenol (**21**)

(*R*)-*N*-(1-(4-Bromophenyl)ethyl)-6-(4-methoxyphenyl)thieno[2,3-*d*]pyrimidin-4-amine (100 mg, 0.228 mmol) was flushed three times with N_2 and dissolved in dry CH_2Cl_2 (2 mL). The reaction was cooled to 0 $^\circ\text{C}$ and BBr_3 in DCM (1 M, 2.5 mL) was added dropwise over 1 h. After a further 3.5 h, the reaction was quenched with H_2O (7.5 mL) and sat. NaHCO_3 solution (5 mL). EtOAc (10 mL) was then added, and the phases separated. The aqueous layer was extracted with EtOAc (5 \times 10 mL), and the combined organic layers were washed with brine (10 mL), dried over anhydrous Na_2SO_4 , filtered, and concentrated in vacuo. The resulting crude material was immobilized on celite and purified by gradient flash chromatography (C18 silica, MeCN/ H_2O , 1:9 to 2:3), resulting in 58 mg (0.137 mmol, 60%) of the desired product as a yellow solid, mp. 144.1–145.4 $^\circ\text{C}$, TLC (MeCN/ H_2O 2:1) $R_f = 0.19$; $[\alpha]_D^{20} = -434$ (c 0.50, EtOH), HPLC purity > 98%, $t_R = 10.69$ min; ^1H NMR (600 MHz, DMSO- d_6) δ : 9.84 (s, 1H), 8.23 (s, 1H), 8.15 (d, $J = 7.7$ Hz, 1H), 7.95 (s, 1H), 7.59–7.47 (m, 4H), 7.44–7.32 (m, 2H), 6.96–6.85 (m, 2H), 5.44 (*p*, $J = 7.1$ Hz, 1H), 1.54 (d, $J = 7.0$ Hz, 3H); ^{13}C NMR (151 MHz, DMSO- d_6) δ : 164.5, 158.1, 155.4, 153.3, 144.3, 139.0, 131.2 (2C), 128.3 (2C), 127.2 (2C), 124.2, 119.6, 117.6, 116.1 (2C), 113.1, 48.7, 40.1, 39.9, 22.4; IR (neat, cm^{-1}): 3321 (O-H), 2973 (Ar C-H), 1586 (N-H), 1495 (Ar C-H), 825 (Ar C-H); HRMS (TOF ES+, m/z): calcd. for $\text{C}_{20}\text{H}_{17}\text{BrN}_3\text{OS}$ [M + H] $^+$: 426.0276, found: 426.0283.

3.5. Bioassays

3.5.1. MIC Measurements

The MIC of compound **1–21** towards *Escherichia coli* (MG1655) and *Staphylococcus aureus* (ATCC29213) was determined following the standards that were recommended by the Clinical and Laboratory Standards Institute (CLSI) for the broth microdilution method [40]. Briefly, the bacterial suspensions were adjusted to 0.5 McFarland standard ($\sim 1 \times 10^8$ colony forming units (CFU)/mL) and diluted 1:200 in Cation-Adjusted Mueller-Hinton Broth (CAMHB, 22.5 mg/mL Ca^{2+} , 11 mg/mL Mg^{2+}). The suspension was subsequently added to polypropylene microtiter plates (100 μL /well, $\sim 5 \times 10^4$ CFU/well) that were already prepared with different concentrations of the various halogenated fused pyrimidines (11 μL /well, two-fold serial dilutions). The plates were incubated at 37 $^\circ\text{C}$ overnight before inspection for visible growth and determination of the MIC values.

3.5.2. *E. coli* and Human TMPK Assay

The inhibition of *Ec*TMPK was determined by Profoldin using the *E. coli* Thymidylate Kinase Assay Kit Plus (ProFoldin, Catalog No. TMK100KE, Hudson, MA, USA), where dTMP was phosphorylated by ATP that was catalyzed by TMPK. The assay was run in 96-well black plates at 36 °C. The formation of ADP was measured by adding a fluorescent dye and measuring the fluorescence emission at 535 nm after excitation at 485 nm. The readout was corrected for emission from the assay cocktail and DMSO. An ADP control assay was also performed to correct for possible interference with ADP detection. Single-point inhibitions were measured at 8.3 μ M inhibitor concentrations. The IC₅₀-values were determined from a similar assay, where 2-fold dilution series from 200 mM to 0.391 mM were used. The assay towards the human enzyme was run similarly but using the Human Thymidylate Kinase Assay Kit Plus-500 (Catalog Number: HTMK500KE, ProFoldin, Hudson, MA, USA).

3.5.3. In Vitro EGFR (ErbB1) Inhibitory Potency

The compounds were supplied in a 10 mM DMSO solution, and enzymatic EGFR (ErbB1) inhibition potency was determined by Invitrogen (ThermoFisher) using their Z'-LYTE[®] assay technology. [49] The compounds were tested for their inhibitory activity at 100 nM in duplicates. The IC₅₀ values that were reported for **1** and **5** are based on the average of 2 titration curves (20 data points), and were calculated from activity data with a four-parameter logistic model using SigmaPlot (Windows Version 12.0 from Systat Software, Inc., Palo Alto, CA, USA). Unless stated otherwise, the ATP concentration that was used was equal to apparent K_M.

3.5.4. Kinase Panel

The compounds were supplied in a 10 mM DMSO solution, and enzymatic kinase inhibition potency was determined by ThermoFisher (Invitrogen, Waltham, MA, USA) using their Z'-LYTE[®] assay technology [49], at 500 nM in duplicates. The ATP concentration that was used was equal to K_m, except when this service was not provided, and other concentrations had to be used.

4. Conclusions

A total of 21 different fused pyrimidines were synthesized and investigated for their antibacterial activity towards *E. coli* and *S. aureus*. The SAR study identified two highly active pyrrolopyrimidines with low MIC values towards *S. aureus*, while none were effective against *E. coli*. Moreover, the SAR study showed that only a minor alteration in the structure affected the activity profoundly, which indicates that the compounds act on a specific intracellular target rather than on the cellular membrane. A hydroxyl group on the *meta*- or *para* position of the 6-aryl unit was found crucial for activity, and heavy halogens (bromo and iodo) in the 4-benzylamine group was strongly potency inducing. Interestingly, when the most potent derivatives were evaluated in combination with the antimicrobial peptide betatide, a four-fold decrease in the MIC value was obtained, a strategy which might be promising for avoiding resistance. The detailed mode of action is currently not known. However, the front runner compound was shown to be a moderately active inhibitor towards *E. coli* TMPK in enzymatic assays and this is also a possible target in *S. aureus*. No major interferences with human kinases were found.

Supplementary Materials: The following are available online at <https://www.mdpi.com/article/10.3390/antibiotics11080984/s1>, Supporting Files: Synthesis of building blocks, NMR spectroscopy and Comparison of TMPK folding. References [12,46,50–53] are cited in the supplementary materials.

Author Contributions: Conceptualization, B.H.H.; synthesis, C.E.O. and F.H.B.; biological studies, C.K.S., L.M.R., A.H.S. and O.E.T.B.; writing—original draft preparation, C.E.O. and B.H.H.; writing—review and editing, C.E.O. and B.H.H.; visualization, E.S.; supervision, P.B., M.O., E.S. and

B.H.H.; funding acquisition, M.O. All authors have read and agreed to the published version of the manuscript.

Funding: This research received funding from Trond Mohn Foundation (TAMIR project).

Institutional Review Board Statement: Not applicable.

Informed Consent Statement: Not applicable.

Data Availability Statement: Data is contained in this article or Supplementary Materials.

Acknowledgments: The support from the Research Council of Norway to the Norwegian NMR Platform (project number 226244/F50) and the Trond Mohn Foundation are highly appreciated. The authors would like to thank Susana Villa Gonzalez and the NTNU Natural Science faculty Mass Spectrometry laboratory for providing instrumentations and data processing software. Roger Aarvik is thanked for technical support.

Conflicts of Interest: There is no conflict of interest.

References

1. Nuding, S.; Frasc, T.; Schaller, M.; Stange, E.; Zabel, L. Synergistic Effects of Antimicrobial Peptides and Antibiotics against *Clostridium difficile*. *Antimicrob. Agents Chemother.* **2014**, *58*, 5719–5725. [[CrossRef](#)]
2. Rajasekaran, G.; Kim, E.Y.; Shin, S.Y. LL-37-derived membrane-active FK-13 analogs possessing cell selectivity, anti-biofilm activity and synergy with chloramphenicol and anti-inflammatory activity. *Biochim. Biophys. Acta Biomembr.* **2017**, *1859*, 722–733. [[CrossRef](#)]
3. Naghmouchi, K.; Le Lay, C.; Baah, J.; Drider, D. Antibiotic and antimicrobial peptide combinations: Synergistic inhibition of *Pseudomonas fluorescens* and antibiotic-resistant variants. *Res. Microbiol.* **2012**, *163*, 101–108. [[CrossRef](#)]
4. Kampshoff, F.; Willcox, M.D.P.; Dutta, D. A Pilot Study of the Synergy between Two Antimicrobial Peptides and Two Common Antibiotics. *Antibiotics* **2019**, *8*, 60. [[CrossRef](#)]
5. Ruden, S.; Rieder, A.; Chis Ster, I.; Schwartz, T.; Mikut, R.; Hilpert, K. Synergy Pattern of Short Cationic Antimicrobial Peptides Against Multidrug-Resistant *Pseudomonas aeruginosa*. *Front. Microbiol.* **2019**, *10*, 2740. [[CrossRef](#)]
6. Rodríguez-Rojas, A.; Nath, A.; El Shazely, B.; Santi, G.; Kim, J.J.; Weise, C.; Kuroopka, B.; Rolff, J. Antimicrobial Peptide Induced-Stress Renders *Staphylococcus aureus* Susceptible to Toxic Nucleoside Analogs. *Front. Immunol.* **2020**, *11*, 1686. [[CrossRef](#)]
7. Zheng, X.; Cao, Q.; Cao, Q.; Mao, F.; Li, X.; Zhu, J.; Lan, L.; Li, J. Discovery of synergistic activity of fluoroquinolones in combination with antimicrobial peptides against clinical polymyxin-resistant *Pseudomonas aeruginosa* DK2. *Chin. Chem. Lett.* **2020**, *31*, 413–417. [[CrossRef](#)]
8. Duong, L.; Gross, S.P.; Siryaporn, A. Developing Antimicrobial Synergy With AMPs. *Front. Med. Technol.* **2021**, *3*, 640981. [[CrossRef](#)]
9. Nedal, A.; Ræder, S.B.; Dalhus, B.; Helgesen, E.; Forstrøm, R.J.; Lindland, K.; Sumabe, B.K.; Martinsen, J.H.; Kragelund, B.B.; Skarstad, K.; et al. Peptides containing the PCNA interacting motif APIM bind to the β -clamp and inhibit bacterial growth and mutagenesis. *Nucleic Acids Res.* **2020**, *48*, 5540–5554. [[CrossRef](#)]
10. Nepal, A.; Ræder, S.B.; Sogaard, C.K.; Haugan, M.S.; Otterlei, M. Broad-Spectrum Antibacterial Peptide Kills Extracellular and Intracellular Bacteria Without Affecting Epithelialization. *Front. Microbiol.* **2021**, *12*, 764451. [[CrossRef](#)]
11. Hoekstra, R.; Dumez, H.; Eskens, F.A.; van der Gaast, A.; Planting, A.S.; de Heus, G.; Sizer, K.C.; Ravera, C.; Vaidyanathan, S.; Bucana, C.; et al. Phase I and pharmacologic study of PKI166, an epidermal growth factor receptor tyrosine kinase inhibitor, in patients with advanced solid malignancies. *Clin. Cancer Res.* **2005**, *11*, 6908–6915. [[CrossRef](#)]
12. Blindheim, F.H.; Malme, A.T.; Dalhus, B.; Sundby, E.; Hoff, B.H. Synthesis and Evaluation of Fused Pyrimidines as *E. coli* Thymidylate Monophosphate Kinase Inhibitors. *ChemistrySelect* **2021**, *6*, 12852–12857. [[CrossRef](#)]
13. Mesa, R.A.; Yasothan, U.; Kirkpatrick, P. Ruxolitinib. *Nat. Rev. Drug Discov.* **2012**, *11*, 103–104. [[CrossRef](#)]
14. Tian, F.; Chen, Z.; Xu, T. Efficacy and safety of tofacitinib for the treatment of chronic plaque psoriasis: A systematic review and meta-analysis. *J. Int. Med. Res.* **2019**, *47*, 2342–2350. [[CrossRef](#)]
15. De Coen, L.M.; Heugebaert, T.S.A.; García, D.; Stevens, C.V. Synthetic Entries to and Biological Activity of Pyrrolopyrimidines. *Chem. Rev.* **2016**, *116*, 80–139. [[CrossRef](#)]
16. Adel, M.; Serya, R.A.T.; Lasheen, D.S.; Abouzid, K.A.M. Pyrrolopyrimidine, A Multifaceted Scaffold in Cancer Targeted Therapy. *Drug Res.* **2018**, *68*, 485–498. [[CrossRef](#)]
17. Liu, Y.; Gong, R.; Liu, X.; Zhang, P.; Zhang, Q.; Cai, Y.-S.; Deng, Z.; Winkler, M.; Wu, J.; Chen, W. Discovery and characterization of the tubercidin biosynthetic pathway from *Streptomyces tubercidicus* NBRC 13090. *Microb. Cell Factories* **2018**, *17*, 131. [[CrossRef](#)]
18. Mohamed, M.S.; El-Domany, R.A.; Abd El-Hameed, R.H. Synthesis of certain pyrrole derivatives as antimicrobial agents. *Acta Pharm.* **2009**, *59*, 145–158. [[CrossRef](#)]
19. Tari, L.W.; Trzoss, M.; Bensen, D.C.; Li, X.; Chen, Z.; Lam, T.; Zhang, J.; Creighton, C.J.; Cunningham, M.L.; Kwan, B.; et al. Pyrrolopyrimidine inhibitors of DNA gyrase B (GyrB) and topoisomerase IV (ParE). Part I: Structure guided discovery and

- optimization of dual targeting agents with potent, broad-spectrum enzymatic activity. *Bioorg. Med. Chem. Lett.* **2013**, *23*, 1529–1536. [CrossRef]
20. Trzoss, M.; Bensen, D.C.; Li, X.; Chen, Z.; Lam, T.; Zhang, J.; Creighton, C.J.; Cunningham, M.L.; Kwan, B.; Stidham, M.; et al. Pyrrolopyrimidine inhibitors of DNA gyrase B (GyrB) and topoisomerase IV (ParE), Part II: Development of inhibitors with broad spectrum, Gram-negative antibacterial activity. *Bioorg. Med. Chem. Lett.* **2013**, *23*, 1537–1543. [CrossRef]
21. Kawatkar, S.P.; Keating, T.A.; Olivier, N.B.; Breen, J.N.; Green, O.M.; Guler, S.Y.; Hentemann, M.F.; Loch, J.T.; McKenzie, A.R.; Newman, J.V.; et al. Antibacterial Inhibitors of Gram-Positive Thymidylate Kinase: Structure–Activity Relationships and Chiral Preference of a New Hydrophobic Binding Region. *J. Med. Chem.* **2014**, *57*, 4584–4597. [CrossRef]
22. Ke, P.-Y.; Kuo, Y.-Y.; Hu, C.-M.; Chang, Z.-F. Control of dTTP pool size by anaphase promoting complex/cyclosome is essential for the maintenance of genetic stability. *Genes Dev.* **2005**, *19*, 1920–1933. [CrossRef]
23. Ahmad, S.I.; Kirk, S.H.; Eisenatark, A. Thymine metabolism and thymineless death in prokaryotes and eukaryotes. *Annu. Rev. Microbiol.* **1998**, *52*, 591–625. [CrossRef]
24. Hernandez, M.Z.; Cavalcanti, S.M.; Moreira, D.R.; de Azevedo Junior, W.F.; Leite, A.C. Halogen atoms in the modern medicinal chemistry: Hints for the drug design. *Curr. Drug Targets* **2010**, *11*, 303–314. [CrossRef]
25. WHO 2021 AWaRe Classification. Available online: <https://www.who.int/publications/i/item/2021-aware-classification> (accessed on 22 June 2022).
26. Kompis, I.; Wick, A. Cheminform Abstract: Synthesis of 4-Halo-Substituted Analogs of Trimethoprim. *Chem. Inf.-Dienst.* **1978**, *9*. [CrossRef]
27. Cosmi, E.V.; Cantini, L.; Monici Preti, P.A.; Di Renzo, G.C.; Abate, F.; Balsotti, G.; Carlomagno, G.; Cirese, E.; Indraccolo, R. Efficacy and tolerability of brodimoprim at two different dosage schedules in the treatment of acute uncomplicated bacterial cystitis: Comparative study vs. pefloxacin. *Eur. J. Obstet. Gynecol. Reprod. Biol.* **1996**, *64*, 207. [CrossRef]
28. Lovell, F.M. The Structure of a Bromine-Rich Marine Antibiotic. *J. Am. Chem. Soc.* **1966**, *88*, 4510–4511. [CrossRef]
29. Fehér, D.; Barlow, R.; McAtee, J.; Hemscheidt, T.K. Highly brominated antimicrobial metabolites from a marine *Pseudoalteromonas* sp. *J. Nat. Prod.* **2010**, *73*, 1963–1966. [CrossRef]
30. Li, C.; Bao, W.; Zhang, H.; Lyu, Z.; Chen, Y.; Guo, Z. Discovery of Brominated Alboflavusins with Anti-MRSA Activities. *Front. Microbiol.* **2021**, *12*, 641025. [CrossRef]
31. Raimondi, M.V.; Cascioferro, S.; Schillaci, D.; Petruso, S. Synthesis and antimicrobial activity of new bromine-rich pyrrole derivatives related to monodeoxyppyoluteorin. *Eur. J. Med. Chem.* **2006**, *41*, 1439–1445. [CrossRef]
32. Labriere, C.; Elumalai, V.; Staffansson, J.; Cervin, G.; Le Norcy, T.; Denardou, H.; Réhel, K.; Moodie, L.W.K.; Hellio, C.; Pavia, H.; et al. Phidianidine A and Synthetic Analogues as Naturally Inspired Marine Antifoulants. *J. Nat. Prod.* **2020**, *83*, 3413–3423. [CrossRef]
33. Labrière, C.; Gong, H.; Finlay, B.B.; Reiner, N.E.; Young, R.N. Further investigation of inhibitors of MRSA pyruvate kinase: Towards the conception of novel antimicrobial agents. *Eur. J. Med. Chem.* **2017**, *125*, 1–13. [CrossRef]
34. Martínez-Botella, G.; Breen, J.N.; Duffy, J.E.S.; Dumas, J.; Geng, B.; Gowers, I.K.; Green, O.M.; Guler, S.; Hentemann, M.F.; Hernandez-Juan, F.A.; et al. Discovery of Selective and Potent Inhibitors of Gram-Positive Bacterial Thymidylate Kinase (TMK). *J. Med. Chem.* **2012**, *55*, 10010–10021. [CrossRef]
35. Mardirossian, M.; Rubini, M.; Adamo, M.F.A.; Scocchi, M.; Saviano, M.; Tossi, A.; Gennaro, R.; Caporale, A. Natural and Synthetic Halogenated Amino Acids—Structural and Bioactive Features in Antimicrobial Peptides and Peptidomimetics. *Molecules* **2021**, *26*, 7401. [CrossRef]
36. Molchanova, N.; Nielsen, J.E.; Sørensen, K.B.; Prabhala, B.K.; Hansen, P.R.; Lund, R.; Barron, A.E.; Jenssen, H. Halogenation as a tool to tune antimicrobial activity of peptoids. *Sci. Rep.* **2020**, *10*, 14805. [CrossRef]
37. Metrangolo, P.; Neukirch, H.; Pilati, T.; Resnati, G. Halogen Bonding Based Recognition Processes: A World Parallel to Hydrogen Bonding. *Acc. Chem. Res.* **2005**, *38*, 386–395. [CrossRef]
38. Wilcken, R.; Zimmermann, M.O.; Lange, A.; Joerger, A.C.; Boeckler, F.M. Principles and Applications of Halogen Bonding in Medicinal Chemistry and Chemical Biology. *J. Med. Chem.* **2013**, *56*, 1363–1388. [CrossRef]
39. Blindheim, F.H.; Olsen, C.E.; Krogh Søgaard, C.; Otterlei, M.; Sundby, E.; Hoff, B.H. Synthetic Strategies towards Imidazopyridinones and 7-Azaoxindoles and their Evaluation as Antibacterial Agents. *Eur. J. Org. Chem.* **2021**, *2021*, 2701–2712. [CrossRef]
40. CLSI. *Methods for Dilution Antimicrobial Susceptibility Tests for Bacteria That Grow Aerobically; Approved Standard*, 9th ed.; CLSI document M07-A9; Clinical and Laboratory Standards Institute: Wayne, PA, USA, 2012.
41. Chaudhary, S.K.; Jeyakanthan, J.; Sekar, K. Structural and functional roles of dynamically correlated residues in thymidylate kinase. *Acta Cryst. D Struct Biol.* **2018**, *74*, 341–354. [CrossRef]
42. Kotaka, M.; Dhaliwal, B.; Ren, J.; Nichols, C.E.; Angell, R.; Lockyer, M.; Hawkins, A.R.; Stammers, D.K. Structures of *S. aureus* thymidylate kinase reveal an atypical active site configuration and an intermediate conformational state upon substrate binding. *Protein Sci.* **2006**, *15*, 774–784. [CrossRef]
43. Sundby, E.; Han, J.; Kaspersen, S.J.; Hoff, B.H. In vitro baselining of new pyrrolopyrimidine EGFR-TK inhibitors with Erlotinib. *Eur. J. Pharm. Sci.* **2015**, *80*, 56–65. [CrossRef]
44. Bugge, S.; Buene, A.F.; Jurisch-Yaksi, N.; Moen, I.U.; Skjønsvell, E.M.; Sundby, E.; Hoff, B.H. Extended Structure–Activity Study of Thienopyrimidine-Based EGFR Inhibitors with Evaluation of Drug-Like Properties. *Eur. J. Med. Chem.* **2016**, *107*, 255–274. [CrossRef]

45. Kaspersen, S.J.; Sørum, C.; Willassen, V.; Fuglseth, E.; Kjøbli, E.; Bjørkøy, G.; Sundby, E.; Hoff, B.H. Synthesis and in vitro EGFR (ErbB1) tyrosine kinase inhibitory activity of 4-*N*-substituted 6-aryl-7*H*-pyrrolo[2,3-*d*]pyrimidine-4-amines. *Eur. J. Med. Chem.* **2011**, *46*, 6002–6014. [[CrossRef](#)]
46. Reiersølmoen, A.C.; Han, J.; Sundby, E.; Hoff, B.H. Identification of fused pyrimidines as interleukin 17 secretion inhibitors. *Eur. J. Med. Chem.* **2018**, *155*, 562–578. [[CrossRef](#)]
47. Traxler, P.; Bold, G.; Brill, W.K.-D.; Frei, J. Preparation of 7*H*-Pyrrolo[2,3-*d*]Pyrimidines as Tyrosine Protein Kinase Inhibitors. WO9702266, 23 January 1997.
48. Kaspersen, S.J.; Sundby, E.; Charnock, C.; Hoff, B.H. Activity of 6-aryl-pyrrolo[2,3-*d*]pyrimidine-4-amines to *Tetrahymena*. *Bioorg. Chem.* **2012**, *44*, 35–41. [[CrossRef](#)]
49. Pollok, B.A.; Hamman, B.D.; Rodems, S.M.; Makings, L.R. Optical Probes and Assays. WO2000066766, 09 November 2000.
50. Liang, X.; Huang, Y.; Zang, J.; Gao, Q.; Wang, B.; Xu, W.; Zhang, Y. Design, synthesis and preliminary biological evaluation of 4-aminopyrazole derivatives as novel and potent JAKs inhibitors. *Bioorg. Med. Chem.* **2016**, *24*, 2660–2672. [[CrossRef](#)]
51. Klečka, M.; Poštová Slavětínská, L.; Hocek, M. Modification of Pyrrolo[2,3-*d*]pyrimidines by C–H Borylation Followed by Cross-Coupling or Other Transformations: Synthesis of 6,8-Disubstituted 7-Deazapurine Bases. *Eur. J. Org. Chem.* **2015**, *2015*, 7943–7961. [[CrossRef](#)]
52. Bugge, S.; Kaspersen, S.J.; Sundby, E.; Hoff, B.H. Route selection in the synthesis of C-4 and C-6 substituted thienopyrimidines. *Tetrahedron* **2012**, *68*, 9226–9233. [[CrossRef](#)]
53. Bugge, S.; Skjønsvell, E.M.; Willumsen, F.B.; Sundby, E.; Hoff, B.H. Improved and Scalable Preparation of 6-Bromo-4-Chlorothieno[2,3-*d*]Pyrimidine. *Chem. Heterocycl. Compd.* **2014**, *50*, 1177–1187. [[CrossRef](#)]